

1
2
3
4
5
6
7
8
9
10
11
12
13
14
15
16
17
18
19

Flavonoid monomers as potent, nontoxic and selective modulators of the breast cancer resistance protein (ABCG2)

Iris L.K. Wong^{a, 1}, Xuezhen Zhu^{a, 1}, Kin-Fai Chan^{a, 1}, Zhen Liu^a, Chin-Fung Chan^a, Tsun Sing Chow^a, Tsz Cheung Chong^a, Man Chun Law^a, Jiahua Cui^b, Larry M.C. Chow^{a,*} and Tak Hang Chan^{a, c,*}

^aDepartment of Applied Biology and Chemical Technology and State Key Laboratory of Chemical Biology and Drug Discovery, Hong Kong Polytechnic University, Hong Kong SAR, China

^bSchool of Environmental Science and Engineering, Shanghai Jiao Tong University, Shanghai 200240, China

^cDepartment of Chemistry, McGill University, Montreal, Quebec, H3A 2K6 Canada

¹These authors contributed equally to this work.

*Co-corresponding authors: Tak Hang Chan and Larry M. C. Chow

For L. M. C. C., Phone: (852)-34008662; Fax: (852)-23649932; E-mail: larry.chow@polyu.edu.hk

For T. H. C., Phone: (852)-34008670; Fax: (852)-23649932; E-mail: hang.chan@polyu.edu.hk

20 **ABSTRACT**

21 We synthesize various substituted triazole-containing flavonoids and identify potent, nontoxic and
22 highly selective BCRP inhibitors. **Ac18Az8**, **Ac32Az19** and **Ac36Az9** possess *m*-
23 methoxycarbonylbenzyloxy substitution at C-3 of the flavone moiety and substituted triazole at C-
24 4' of B-ring. They show low toxicity (IC_{50} towards L929 > 100 μ M), potent BCRP-inhibitory
25 activity (EC_{50} = 1-15 nM) and high BCRP selectivity (BCRP selectivity over MRP1 and P-gp >
26 67-714). They inhibit the efflux activity of BCRP, elevate the intracellular drug accumulation, and
27 restore the drug sensitivity of BCRP-overexpressing cells. Like Ko143, **Ac32Az19** remarkably
28 exhibits 100% 5D3 shift, indicating that it can bind and cause conformational change of BCRP.
29 Moreover, it significantly reduces the abundance of functional BCRP dimer/oligomer by half to
30 retain more mitoxantrone in the BCRP-overexpressing cell line and that may account for its
31 inhibitory activity. They are promising candidates to be developed into combination therapy to
32 overcome MDR cancers with BCRP overexpression.

33

34 Keywords: Flavonoids, Triazole, Breast Cancer Resistance Protein, BCRP inhibitor, Multidrug
35 Resistance

36

37 1. INTRODUCTION

38 Multidrug resistance (MDR) is a major obstacle in clinical treatment in which many
39 cancers develop resistance towards different kinds of drugs and eventually result in
40 chemotherapy failure. Resistance to chemotherapy has been associated with the overexpression
41 of ATP-binding cassette (ABC) transporters in tumor cell membranes that actively expel anti-
42 cancer drugs from the cytoplasm and cause the intracellular drug concentration below the
43 therapeutic level.

44 Breast cancer resistance protein (BCRP; ABCG2) is one of three major members of the
45 ABC transporter protein family besides P-glycoprotein (P-gp; ABCB1) and multidrug
46 resistance associated protein 1 (MRP1; ABCC1).¹⁻⁴ BCRP, unlike dimeric P-gp and MRP1, is a
47 72 kDa half transporter and consists of only one cytosolic nucleotide-binding domain (NBD) and
48 one transmembrane domain (TMD).⁵ BCRP has been reported to form a dimer or oligomer when
49 it functions as a transporter.⁶⁻⁸ BCRP is found in various human cancers.⁹⁻¹⁶ Its level is associated
50 with clinical drug resistance and lower survival rate.⁹⁻¹⁶ Since its discovery in 1998,¹⁷⁻¹⁹ numerous
51 anticancer drugs including methotrexate,²⁰ mitoxantrone,²¹ topotecan,²² irinotecan²³ and its active
52 metabolite SN-38,²⁴ as well as some tyrosine kinase inhibitors (TKIs)²⁵ have been identified as
53 BCRP substrates. The approach of co-administration of a potent inhibitor of ABC transporter with
54 an anticancer drug to overcome MDR has been evaluated in several clinical trials.²⁶⁻²⁹ Several
55 phase III clinical trials of P-gp inhibitors³⁰⁻³² all ended with negative results. One factor for the
56 lack of success may be the fact that none of the above clinical trials had patient selection based on
57 prospective evaluation of the expression of the drug transporters. In the trials that evaluated P-gp
58 inhibitors in non-small cell lung cancer, for example, transporters such as MRP1 or BCRP rather
59 than P-gp may have accounted for the drug resistance.³³ Inhibitors that targeted P-gp would have

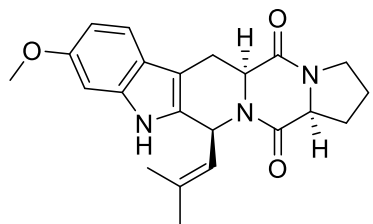
60 failed to overcome MDR due to overexpression of MRP1 or BCRP. Additional factors suggested
61 for the lack of success in this strategy of overcoming MDR are: (1) enhanced toxicity at non-target
62 site due to the inhibitor, (2) drug-drug interaction of the anticancer drug with the inhibitor leading
63 to enhanced toxicity and (3) the inhibitor may adversely modify drug distribution in solid tumors.³⁴
64 It is suggested that further improvement of inhibitors of ABC transporters should focus on potency,
65 specificity and safety.³⁰

66 Fumitremorgin C (**Figure 1**) was the first identified BCRP inhibitor with effective
67 concentration (EC₅₀) around 1-5 μM.^{23,35} However, it was neurotoxic and had been precluded from
68 clinical development.³⁵ In later studies, one of the analogues of fumitremorgin C, Ko143 (**Figure**
69 **1**)³⁶ was identified as a potent and selective inhibitor of BCRP with EC₅₀ around 10 nM.³⁶ It was
70 not stable in mouse plasma when administered p.o. to inhibit intestinal BCRP. Tariquidar (**Figure**
71 **1**)³⁷, a potent P-gp inhibitor, has also been reported to inhibit BCRP with EC₅₀ around 100 nM.³⁸
72 Recently, 2,4,6-substituted quinazolines (with EC₅₀ = 20-71 nM),³⁹ 2,4-disubstituted
73 pyridopyrimidines (with EC₅₀ = 37 nM)⁴⁰ and 4-anilino-2-pyridylquinazolines and -pyrimidines
74 (with EC₅₀ = 21 nM)⁴¹ have been reported to be highly potent and nontoxic inhibitors of BCRP.
75 More recently, indenoindole inhibitors of BCRP with EC₅₀ of 24 nM⁴² and 210 nM⁴³ for inhibiting
76 mitoxantrone efflux have been reported.

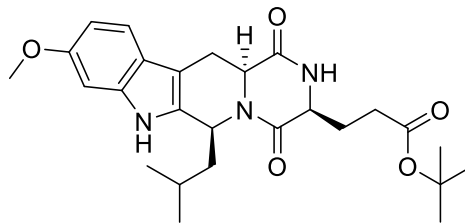
77 Flavonoids are abundant in fruits, vegetables, tea and herbal products. They possess various
78 beneficial properties including antioxidant, anti-inflammatory, antiviral and anticancer
79 properties⁴⁴⁻⁴⁸ and are commonly regarded as safe substances for human consumption. Many
80 natural flavonoids have been found to exhibit moderately weak activity in modulating ABC
81 transporters with EC₅₀ in the micromolar regime.⁴⁹ A structure activity relationship (SAR) study

82 of flavonoids as BCRP inhibitors led to the suggestion that the inhibition may involve, in part, the
83 binding of flavonoids with the NBD of BCRP.⁵⁰ In order to potentiate the MDR modulation effect
84 of flavonoids, we have previously found that flavonoid dimers of general structure I with 4-5
85 polyethylene glycol (PEG) units (**Figure 1**) were promising P-gp and MRP1 inhibitors with
86 nanomolar EC₅₀ values (70 to 170 nM).⁵¹⁻⁵⁵ Recently, we have successfully employed the copper
87 (I) catalyzed Huisgen 1,3-dipolar cycloaddition reaction between alkyne (**AcN**) and azide (**AzM**)
88 to efficiently synthesize triazole-linked flavonoid dimers (**AcNAzM** and **AcN(AzM)₂**) as potent
89 MRP1 and BCRP inhibitors.^{56, 57} Thus, it was found that compound **Ac3Az11** (**Figure 1**) was
90 potent MRP1 inhibitor (EC₅₀ = 53 nM)⁵⁶ and compound **Ac22(Az8)₂** (**Figure 1**) was potent BCRP
91 inhibitor (EC₅₀ = 1-2 nM).⁵⁷ The latter compound was found to inhibit the BCRP-ATPase activity
92 and block the efflux activity of BCRP thus elevating the intracellular drug accumulation. The
93 biochemical studies suggested that it bound to the same drug-binding site, consistent with the cryo-
94 EM structures revealed for BCRP in complex with substrate/inhibitor.⁵⁸⁻⁶⁰

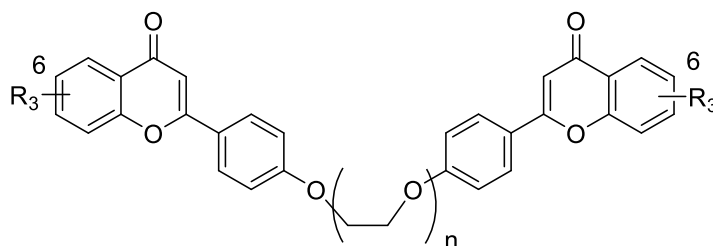
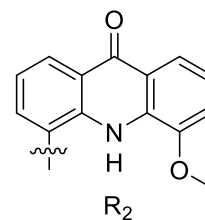
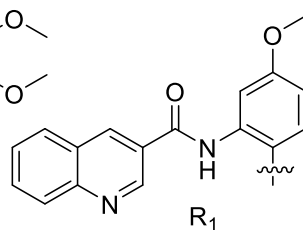
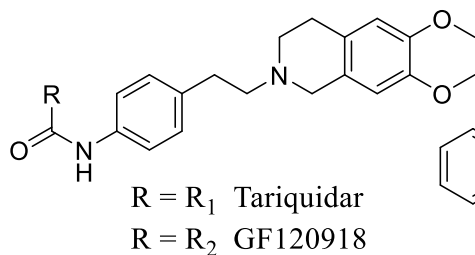
95 In the BCRP study,⁵⁷ it was observed that compounds which contained no flavonoid moiety
96 were essentially nonactive (EC₅₀ > 1000 nM). Furthermore, it seemed that flavonoid dimers
97 derived from **Az8** or **Az9** were highly potent irrespective of the **Ac** component to which they were
98 coupled, with EC₅₀ ranged from 1 to 24 nM.⁵⁷ We are therefore interested to examine monomeric
99 flavonoids with structural motif analogous to **Az8** or **Az9** to see if they can exhibit potent inhibitory
100 activity against BCRP. Such monomeric flavonoids would have the advantage of having lower
101 molecular weights than the corresponding dimers and are likely to be more druggable.



Fumitremorgin C

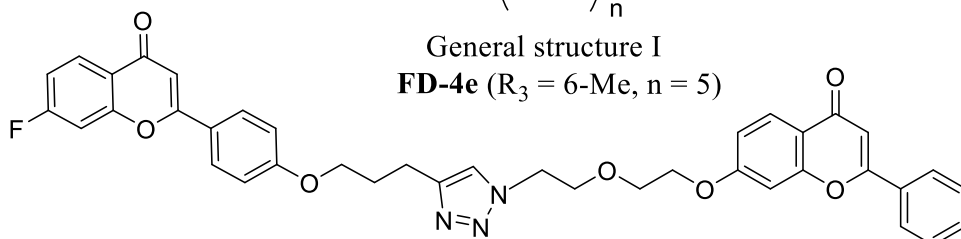


Ko143

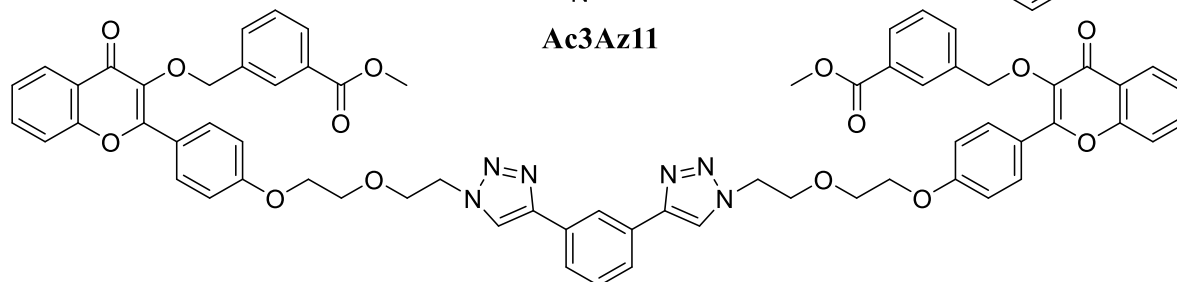


General structure I

FD-4e (R₃ = 6-Me, n = 5)



Ac3Az11



Ac22(Az8)₂

102

103 **Figure 1.** Chemical structures of fumitremorgin C, Ko143, tariquidar, GF120918, general

104 structure I, **Ac3Az11** and **Ac22(Az8)₂**.

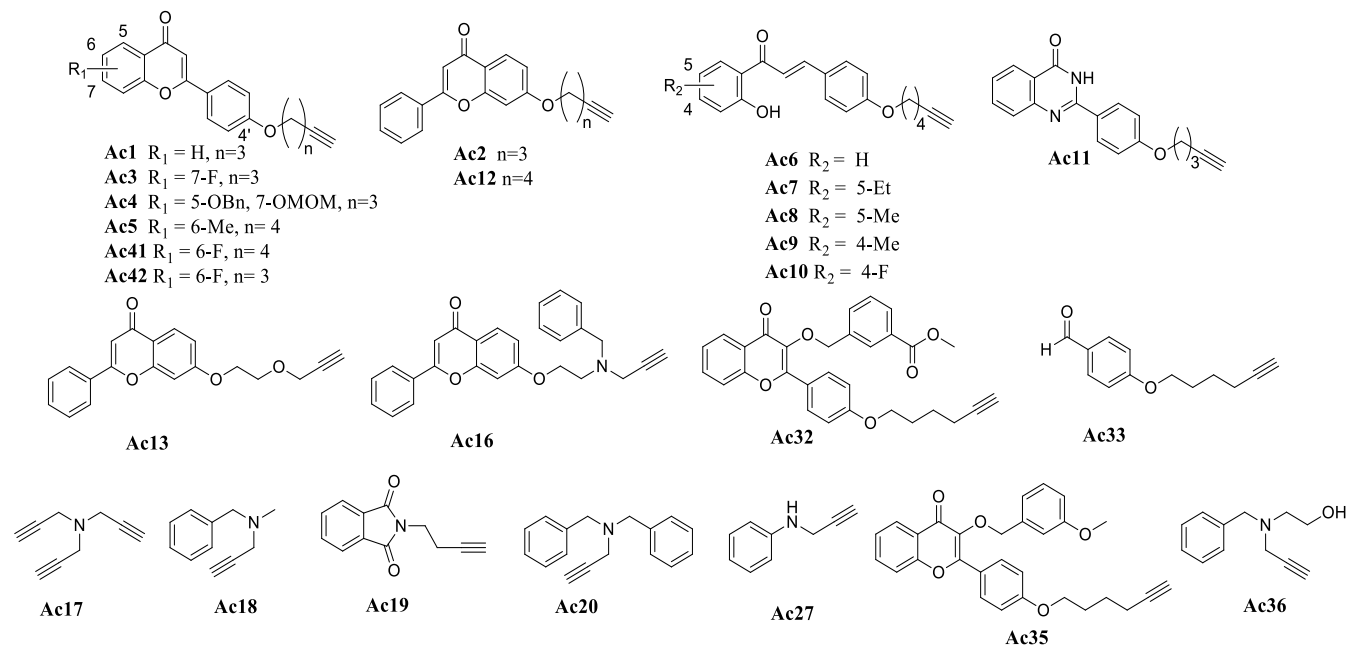
105

106 2. RESULTS

107 2.1 Design and synthesis of flavonoid monomers

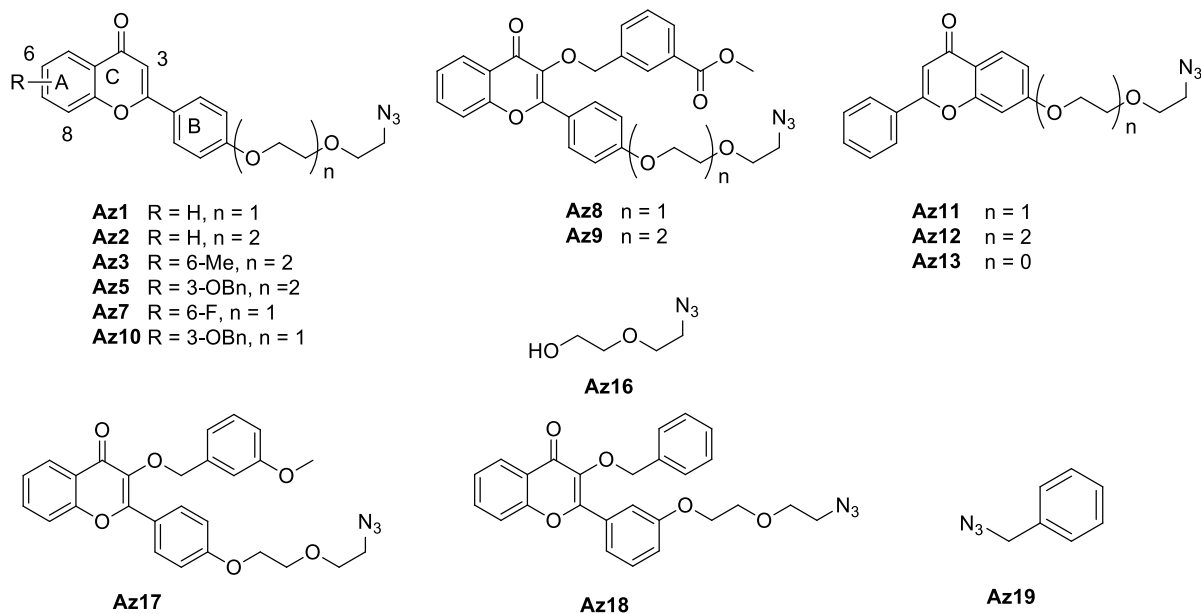
108 The alkynes **Ac1-Ac13**, **Ac16**, **Ac33**, **Ac35** and **Ac42** (**Figure 2**) and the azides **Az1-Az3**,
109 **Az5**, **Az7-Az13**, **Az17** and **Az18** (**Figure 3**) are conveniently prepared according to the procedure
110 described in the previous study.^{56, 57} From previous studies, the most potent triazole-containing
111 homodimers for selectively inhibiting BCRP contain *m*-methoxycarbonylbenzyloxy modification
112 at the C-ring of flavone moieties, conjugate the linker at C-4' of B ring and are longer than 21
113 atoms in linker length.⁵⁷ For the present study of monomers, we have maintained the conjugation
114 at C-4' of B ring. In some cases, the *m*-methoxycarbonylbenzyloxy group has been modified to
115 benzyloxy (**Az18**) or *m*-methoxybenzyloxy (**Ac35** and **Az17**) to probe the effect of the *m*-
116 methoxycarbonyl group on the activity. Monomers of various R (R₁ and R₂) substituents (F, Me,
117 OMOM, OBn...) in the A ring, different linkers (polymethylene, PEG or aminoethoxy) with
118 different lengths, are conveniently available from previous study^{56, 57} and are used as such to
119 examine the effect of substituents and linkers on activity. For non-flavonoid containing alkynes
120 (**Ac17-27**, **Ac33** and **Ac36**) and azides (**Az16** and **Az19**), they are chosen mainly because they are
121 either commercially available or easily synthesized. Three more novel **AcN** monomers, **Ac32**,
122 **Ac41** and **Ac43** are synthesized. For **Ac32** and **Ac41**, the intermediates **1a** and **2a** are alkylated
123 respectively with the halogenated reagents **1b** and **2b** to afford the desired compounds (**Scheme**
124 **1**). For **Ac43**, the hydroxylated flavone **3a** is coupled with *tert*-butyl benzyl(2-
125 hydroxyethyl)carbamate **3b** under Mitsunobu condition and the Boc group of the coupled product
126 is removed under acidic condition to furnish the desired product (**Scheme 1**). With one compound
127 bearing an acetylene group (**AcN**) and another compound bearing an azido group (**AzM**), a

128 triazole-containing flavonoid monomers could be easily obtained by employing the CuAAC
 129 reaction. (Scheme 2).



130

131 **Figure 2.** Structures of AcN compounds.

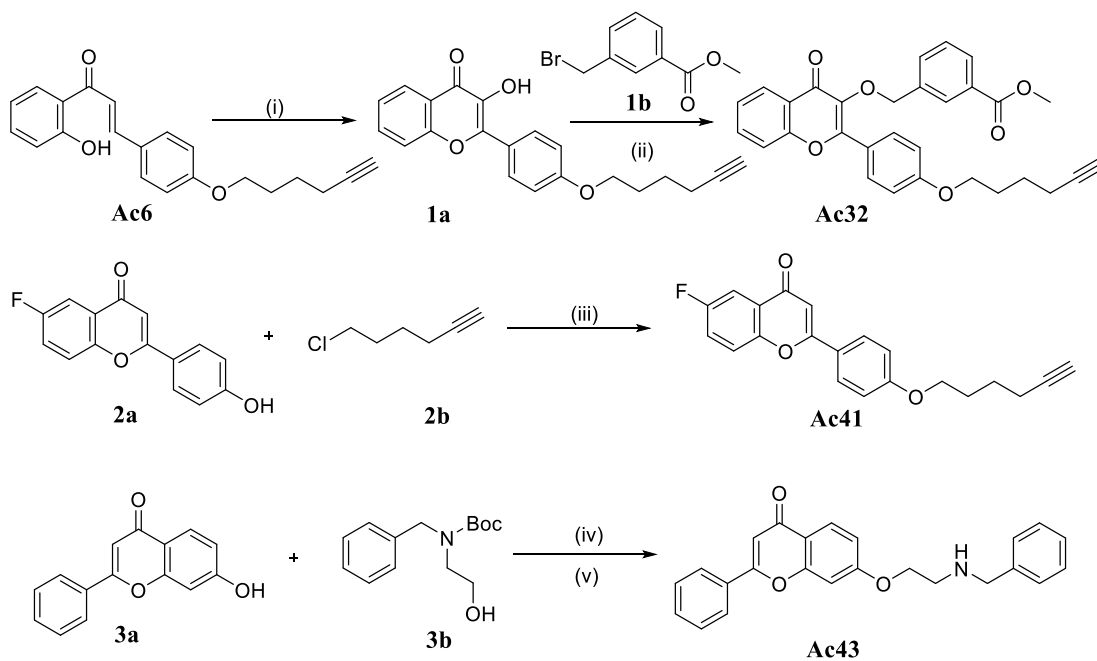


132

133 **Figure 3.** Structures of AzM compounds.

134

135 **Scheme 1.** Synthesis of Ac32, Ac41, Ac43.^a



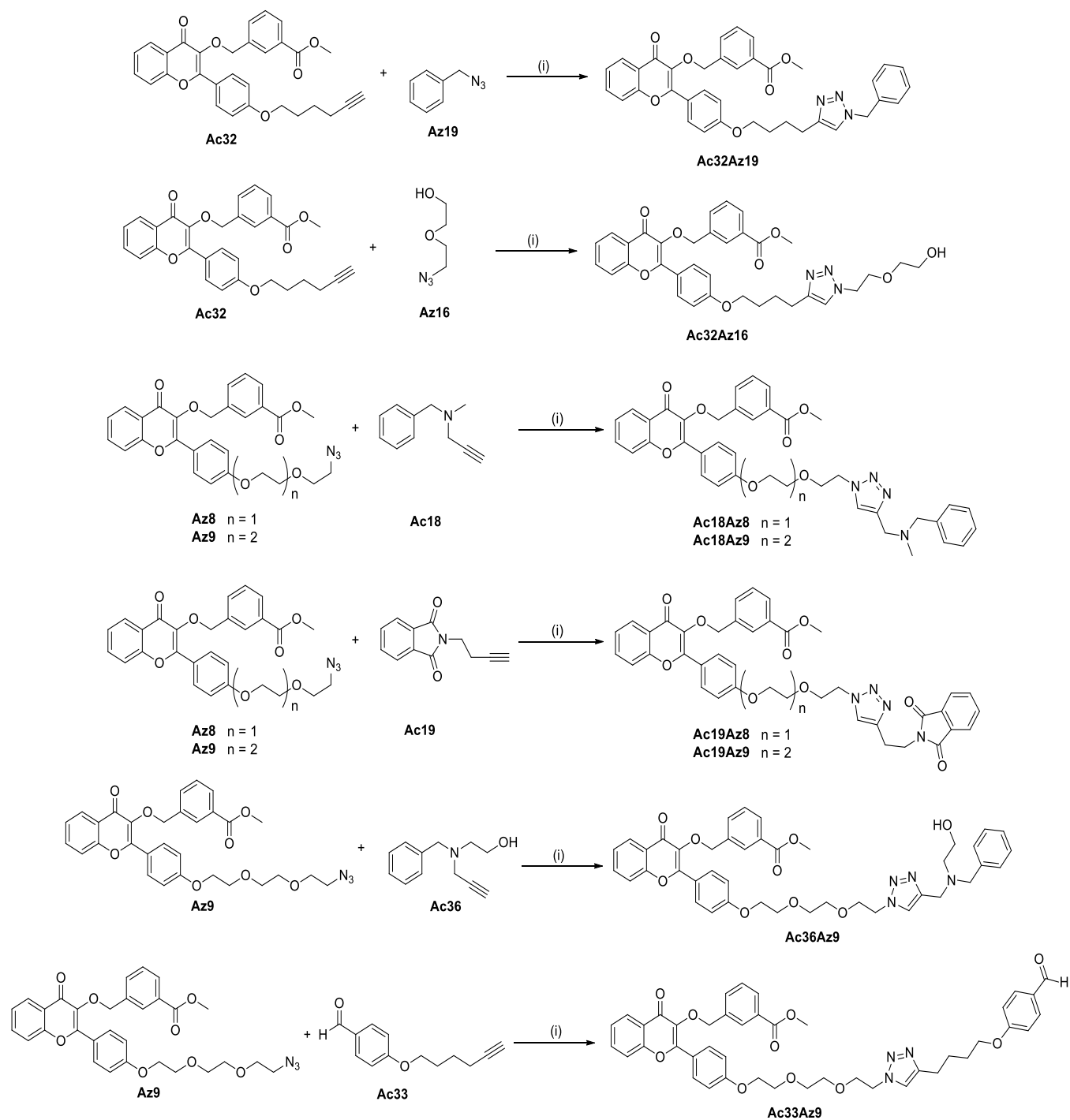
137 ^a Reagents and condition: (i) H₂O₂, KOH, acetone, reflux 6 hr; (ii) methyl 3-

138 (bromomethyl)benzoate, K₂CO₃, acetone reflux 12 hr; (iii) K₂CO₃, KI, DMF, reflux, 2 hr; (iv)

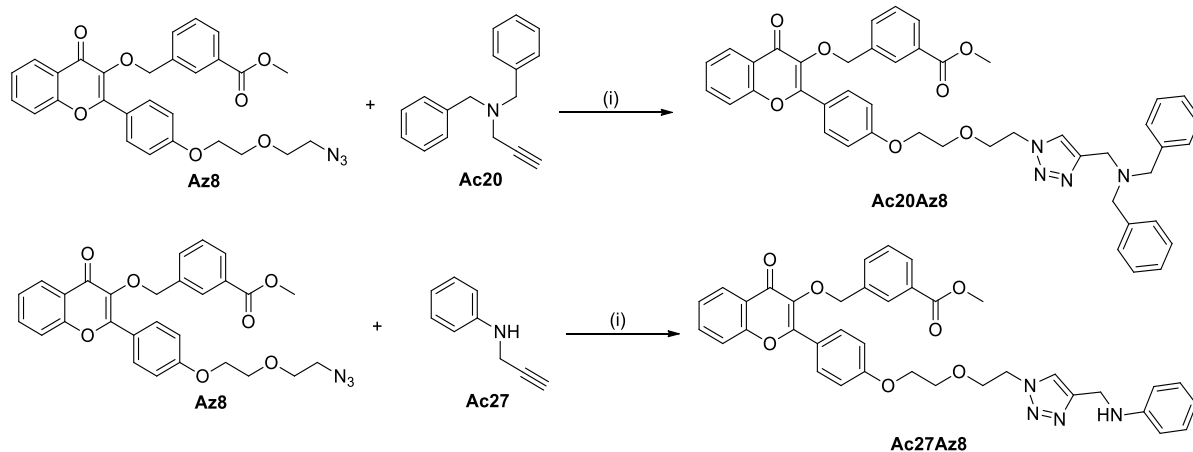
139 PPh₃, DIAD, THF; (v) TFA, DCM.

140

141 **Scheme 2.** Synthesis of triazole bearing flavonoid monomers.^a



142



143

144 ^a Reagents and condition: (i) cat. Cu(PPh₃)₃Br, THF, reflux, 12 hr.

145 2.2. Biological assay results

146 2.2.1. SAR of flavonoid monomers and BCRP-inhibitory activity

147 For screening of BCRP-modulating activity of flavonoid monomers (**AcN** or **AzM**), BCRP-
 148 transfected human embryonic kidney cell line HEK293/R2 is used (**Table 1**). EC₅₀ at which
 149 modulator can reduce IC₅₀ of cell line toward a drug by half, is used to discriminate the BCRP
 150 inhibitory potency. The flavonoid monomers would be considered as potent BCRP inhibitors if
 151 they exhibit EC₅₀ values less than 100 nM (**Table 1**).

152 In the 25-member of **AcN** library (**Table 1**), 19 compounds are found to be nonactive with
 153 EC₅₀ values greater than 1000 nM. Of those, six compounds (**Ac17-Ac20**, **Ac27** and **Ac33**)
 154 containing no flavone moiety do not show any BCRP-modulating activity, indicating that the
 155 presence of flavone moiety is necessary for BCRP inhibition. Secondly, replacing the flavone
 156 structure with a chalcone (**Ac6-Ac10**) or a quinazolinone moiety (**Ac11**) also show no BCRP
 157 inhibitory potency. Thus, flavone but not chalcone or quinazolinone moiety is an important
 158 pharmacophore for BCRP modulation. In order to understand the SAR for inhibiting BCRP
 159 activity, we have (1) introduced various substituents at C-5, C-6 or C-7 on A-ring or at C-3 on C-

160 ring of the flavonoid moiety; (2) synthesized different linker length between the flavone and alkyne;
161 (3) located the linker at either C-4' of ring B or C-7 of ring A and (4) designed the linker with a
162 *N*-atom bearing benzyl substituent. It is found that linker conjugated at C-7 position of A-ring
163 (**Ac2**, **Ac12**, **Ac13**, **Ac16** and **Ac43**) is not preferred as it results in $EC_{50} > 1000$ nM as compared
164 to conjugation site at C-4' position of B-ring. Moreover, either **Ac16** or **Ac43** having *N*-benzyl
165 substitution at the linker is unfavorable for BCRP modulation. Among the remaining **AcN**
166 monomers with both flavone moiety and C-4' linker conjugation, 5-, 6- or 7-substitutions at A-
167 ring (**Ac3**, **Ac4**, **Ac41** and **Ac42**) or 3-substitution at C-ring (**Ac32** and **Ac35**), they have improved
168 BCRP-inhibitory activity with EC_{50} ranged from 44 nM to 417 nM as compared to unsubstituted
169 **Ac1** monomer ($EC_{50} > 1000$ nM). Moreover, substituent F- at C-6 of A ring such as **Ac41** or **Ac42**
170 ($EC_{50} = 240$ to 417 nM) is more potent than **Ac5** which has CH_3 - substitution ($EC_{50} > 1000$ nM).
171 **Ac32**, containing *m*-methoxycarbonylbenzyloxy substitution at C-3 of C-ring, is the most potent
172 inhibitor with EC_{50} of 44 nM. When the carbonyl group is removed from **Ac32** to become *m*-
173 methoxybenzyloxy substituted **Ac35** ($EC_{50} = 261$ nM), a 6-fold decrease in BCRP inhibitory
174 activity is noted.

175 In the 15-member **AzM** library, **Az16** and **Az19** without flavone moiety are the poorest
176 inhibitor with $EC_{50} > 1000$ nM. Thirteen compounds possess EC_{50} ranging from 8.5 nM to 840
177 nM. Five of them, **Az5**, **Az8-Az10** and **Az17**, are potent BCRP modulators with $EC_{50} < 100$ nM.
178 Like **Ac32**, **Az9** containing *m*-methoxycarbonylbenzyloxy substitution is the most active one with
179 EC_{50} less than 10 nM (**Table 1**). However, when the *m*-methoxycarbonyl group is removed from
180 **Az9** to become benzyloxy substituted **Az5** ($EC_{50} = 52$ nM), there is a 6-fold decrease in potency.
181 The same decrease is found for **Az8** ($EC_{50} = 80$ nM) and **Az18** ($EC_{50} = 169$ nM). The *m*-ester group
182 at the benzyloxy substituent in C-ring appears to enhance the BCRP inhibitory activity. Other than

183 modification at the C-ring, linker length between C-4' position and the azide moiety also play a
184 role in controlling the BCRP-modulating activity. **Az9** ($EC_{50} = 8.5$ nM) with 2 PEG units shows
185 9.4-fold higher BCRP inhibitory activity than **Az8** ($EC_{50} = 80$ nM) which possesses 1 PEG unit
186 (**Table 1**).

Table 1. BCRP-modulating activity of flavonoid AcN and AzM monomers.

AcN monomers	Structure	EC ₅₀ (nM) for reversing BCRP-mediated topotecan resistance in HEK293/R2	AcN monomers	Structure	EC ₅₀ (nM) for reversing BCRP-mediated topotecan resistance in HEK293/R2	AzM monomers	Structure	EC ₅₀ (nM) for reversing BCRP-mediated topotecan resistance in HEK293/R2
Ac1		>1000	Ac16		>1000	Az1		365.0 ± 135.4
Ac2		>1000	Ac17		>1000	Az2		362.5 ± 47.6
Ac3		325.0 ± 100.3	Ac18		>1000	Az3		750.0 ± 150.4
Ac4		200.5 ± 36.9	Ac19		>1000	Az5		52.0 ± 17.6
Ac5		>1000	Ac20		>1000	Az7		840.0 ± 5.8
Ac6		>1000	Ac27		>1000	Az8		80.3 ± 24.1
Ac7		>1000	Ac32		43.8 ± 12.6	Az9		8.5 ± 1.3
Ac8		>1000	Ac33		>1000	Az10		45.3 ± 9.6
Ac9		>1000	Ac35		261.3 ± 11.3	Az11		222.5 ± 49.2
Ac10		>1000	Ac41		240.0 ± 40.1	Az12		176.7 ± 16.4
Ac11		>1000	Ac42		416.5 ± 22.6	Az13		212.5 ± 28.4
Ac12		>1000	Ac43		>1000	Az16		>1000
Ac13		>1000	Ko143		8.7 ± 4.9	Az17		76.0 ± 19.2
 R = N ₃ or ≡			 2.5 ± 1.5			Az18		169.0 ± 31.1
						Az19		>1000

189 A total of 40 flavonoid monomers are synthesized and their BCRP-modulating activities are
190 determined. EC₅₀ value is used to differentiate the reversal potency of these flavonoid monomers.
191 EC₅₀ value is presented as mean ± standard error of mean. N = 3-4 independent experiments.
192 Ko143 and **Ac22(Az8)₂** are BCRP-specific inhibitors and used as positive controls.

193 **2.2.2** BCRP-modulating activity and BCRP selectivity of triazole derivatives of **Ac32**, **Az8** and 194 **Az9**

195 **Ac32**, **Az8** and **Az9** are promising BCRP inhibitors and possess the important pharmacophore
196 *m*-methoxycarbonylbenzyloxy substitution at the C-3 of C-ring. However, they are still not good
197 candidates for future use. Although **Az9** is quite active with EC₅₀ of 8.5 nM (**Table 1**), it causes
198 moderate toxicity towards L929 (IC₅₀ = 28.4 μM, **Table 2**). **Ac32** and **Az8** are not potent enough
199 with EC₅₀ of 44 nM and 80 nM (**Table 1**). Here, using the Huisgen 1,3-dipolar cycloaddition
200 reaction, we introduce a triazole ring and various side chains to **Ac32**, **Az8** and **Az9** to further
201 study their BCRP modulation in both HEK293/R2 and MCF7MX100 cells. Like their precursor
202 compounds, these triazole-containing derivatives are all active against BCRP in both cell lines
203 (EC₅₀ = 1.4 to 160 nM, **Table 2**). They are all relatively nontoxic as measured by their cytotoxicity
204 towards the normal mouse fibroblast L929 cells (IC₅₀ = 13.3 to >100 μM, **Table 2**). They are less
205 active as P-gp inhibitors (EC₅₀ = 298 to >1000 nM, **Table 2**) and as MRP1 inhibitors (EC₅₀ = 865
206 to >1000 nM, **Table 2**), indicating that they are all more BCRP-selective (BCRP selectivity over
207 P-gp > 6-286 and BCRP selectivity over MRP1 > 6-714) (**Table 2**).

208 In general, BCRP inhibitory potency of **Ac32**, **Az8** and **Az9** derivatives are significantly
209 improved after introduction of the triazole structure. Thus, **Ac32Az16**, **Ac32Az19**, **Ac18Az8**,
210 **Ac20Az8**, **Ac27Az8**, **Ac18Az9**, **Ac33Az9** and **Ac36Az9** are all more potent than their precursors
211 **Ac32**, **Az8** and **Az9** respectively (**Table 2**), suggesting that the triazole plays a positive role in

212 enhancing BCRP inhibition. The only exceptions are **Ac19Az8** and **Ac19Az9**. The presence of the
213 phthalimide structure appears to have a slight negative effect, leading to no overall improvement
214 in activity over the precursors. Other than phthalimide, other substituents attached to the triazole
215 structure give highly active BCRP inhibitors. The most potent is **Ac36Az9** with $EC_{50} = 1.4$ and
216 1.6 nM for the two *in vitro* assays (in comparison with Ko143, the EC_{50} are 8.7 and 9.0 nM). Two
217 other compounds, **Ac32Az19** ($EC_{50} = 7.0$ and 6.0 nM) and **Ac18Az8** ($EC_{50} = 14.9$ and 3.5 nM) are
218 comparable to Ko143 in potency.





219 These three triazole-containing derivatives, **Ac18Az8**, **Ac32Az19** and **Ac36Az9** are chosen
220 for further mechanistic characterization because of their high potency. They also show high BCRP
221 selectivity over P-gp and MRP1 (BCRP selectivity > 67 - 714 comparable to BCRP selectivity of
222 Ko143 = 118 - 224). More importantly, they are nontoxic as their IC_{50} values are greater than 100
223 μ M towards L929 (**Table 2**) whereas Ko143 shows moderate toxicity ($IC_{50} = 31$ μ M).

224

225

Table 2. EC₅₀ (nM) of Ac32, Az8 and Az9 triazole-containing derivatives for reversing MDR and their BCRP-selectivity.

Cpds	Structure	Cytotoxicity (IC ₅₀ , μM) L929	EC ₅₀ (nM) for reversing MDR				BCRP selectivity			
			HEK293/R2 BCRP-mediated topotecan resistance	MCF7-MX100 BCRP-mediated topotecan resistance	LCC6MDR P-gp-mediated paclitaxel resistance	2008MRP1 MRPI-mediated DOX resistance	Relative to P-gp inhibition		Relative to MRPI inhibition	
			HEK293/R2	MCF7-MX100	LCC6MDR	2008MRP1	HEK293/R2	MCF7-MX100	HEK293/R2	MCF7-MX100
Ac32		>100	43.8 ± 12.6	33.7 ± 3.8	820.7 ± 99.0	1000 ± 0.0	19	24	23	30
Ac32Az16		13.3 ± 2.5	10.0 ± 4.5	27.4 ± 9.6	606.3 ± 62.8	>1000	61	22	100	36
Ac32Az19		>100	7.0 ± 0.2	6.0 ± 3.4	670.0 ± 70.2	>1000	96	112	143	167
Az8		67.5 ± 2.0	80.3 ± 24.1	49.7 ± 19.1	>1000	>1000	12	20	12	20
Ac18Az8		>100	14.9 ± 5.3	3.5 ± 1.0	>1000	>1000	67	286	67	286
Ac19Az8		>100	46.4 ± 12.7	96.7 ± 26.8	>1000	>1000	22	10	22	10
Ac20Az8		>100	32.0 ± 8.0	29.8 ± 11.2	>1000	>1000	31	34	31	34
Ac27Az8		>100	26.4 ± 6.7	44.3 ± 14.7	>1000	>1000	38	23	38	23
Az9		28.4 ± 7.8	8.5 ± 1.3	16.8 ± 4.1	297.5 ± 50.4	>1000	35	18	118	60
Ac18Az9		>100	16.2 ± 8.2	28.2 ± 8.9	830.0 ± 114.7	>1000	51	29	62	35
Ac19Az9		>100	160.0 ± 61.8	ND	>1000	>1000	6	ND	6	ND
Ac33Az9		37.8 ± 4.8	18.9 ± 6.0	38.2 ± 15.6	>1000	865.0 ± 104	53	26	46	23
Ac36Az9		>100	1.4 ± 0.5	1.6 ± 0.8	308.5 ± 25.6	>1000	220	193	714	625
Ko143		31.4 ± 1.6	8.7 ± 2.2	9.0 ± 1.5	1060.0 ± 120.1	1950.0 ± 251	122	118	224	217

227		BCRP-selectivity > 200
		BCRP-selectivity = 101-200
		BCRP-selectivity = 50-100
		BCRP-selectivity < 50

228 Potent monomers including **Ac32**, **Az8** and **Az9** are further potentiated by formation of a triazole
 229 with various side chains. The BCRP-, P-gp and MRP1-modulating activities of these new
 230 derivatives are studied using BCRP-overexpressing cell lines HEK293/R2 and MCF7-MX100, P-
 231 gp-overexpressing cell line LCC6MDR and MRP1-overexpressing cell line 2008MRP1. EC₅₀
 232 value is presented as mean ± standard error of mean. N = 3-4 independent experiments. Selectivity
 233 index of an inhibitor for transporter A over transporter B as the inverse ratio of EC₅₀ of the inhibitor
 234 for transporter A over the EC₅₀ of the same inhibitor for transporter B. The NMR data of these
 235 compounds are shown in Supporting Information.

236 2.2.3 **Ac18Az8**, **Ac32Az19** and **Ac36Az9** selectively reverse mitoxantrone resistance in BCRP- 237 overexpressed cell line

238 Mitoxantrone is an overlap substrate among BCRP, MRP1 and P-gp transporters.⁶¹ In order
 239 to further confirm the BCRP selectivity of **Ac18Az8**, **Ac32Az19** and **Ac36Az9**, mitoxantrone
 240 cytotoxicity with or without these inhibitors is determined using BCRP-, MRP1- and P-gp-
 241 overexpressed cell lines. **Ac18Az8**, **Ac32Az19** and Ko143 potently modulate BCRP-mediated
 242 mitoxantrone resistance in HEK293/R2 with EC₅₀ less than 20 nM (**Table 3**). **Ac18Az8** and
 243 **Ac32Az19** exhibit relatively weak MRP1- or P-gp modulating activities with EC₅₀ ranged from
 244 644 nM to 886 nM and their BCRP selectivity over P-gp and MRP1 range from 38 to 68. Thus,
 245 mitoxantrone sensitization assay demonstrates that **Ac18Az8** and **Ac32Az19** have higher efficacy
 246 for BCRP than for P-gp and MRP1.

247 **Table 3. Ac18Az8, Ac32Az19 and Ac36Az9 selectively reverse mitoxantrone resistance in**
 248 **BCRP-overexpressed cell line but not MRP1- or P-gp overexpressed cell lines.**

Compounds	EC ₅₀ (nM) for reversing mitoxantrone resistance			BCRP selectivity	
	BCRP- overexpressed	P-gp- overexpressed	MRP1- overexpressed	Relative to P-gp inhibitory activity	Relative to MRP1 inhibitory activity
	HEK293/R2	LCC6MDR	2008MRP1		
Ac18Az8	17 ± 4	644 ± 161	681 ± 151	38	40
Ac32Az19	13 ± 3	673 ± 119	886 ± 92	52	68
Ac36Az9	165 ± 15	817 ± 127	592 ± 108	5	4
Ko143	5 ± 1	943 ± 233	1800 ± 201	189	360

250 Mitoxantrone is an overlap substrate among BCRP, MRP1 and P-gp transporters. EC₅₀ values of
 251 **Ac18Az8, Ac32Az19, Ac36Az9** and Ko143 for reversing mitoxantrone resistance in HEK293/R2,
 252 LCC6MDR and 2008MRP1 are determined. N = 2-4 independent experiments. EC₅₀ values are
 253 presented as mean ± standard error of mean. Selectivity index of an inhibitor for transporter A over
 254 transporter B as the inverse ratio of EC₅₀ of the inhibitor for transporter A over the EC₅₀ of the
 255 same inhibitor for transporter B.

256 **2.2.4 BCRP inhibitors Ac18Az8, Ac32Az19 and Ac36Az9 increase retention of BCRP-substrates**
 257 **by inhibiting efflux in HEK293/R2 cells**

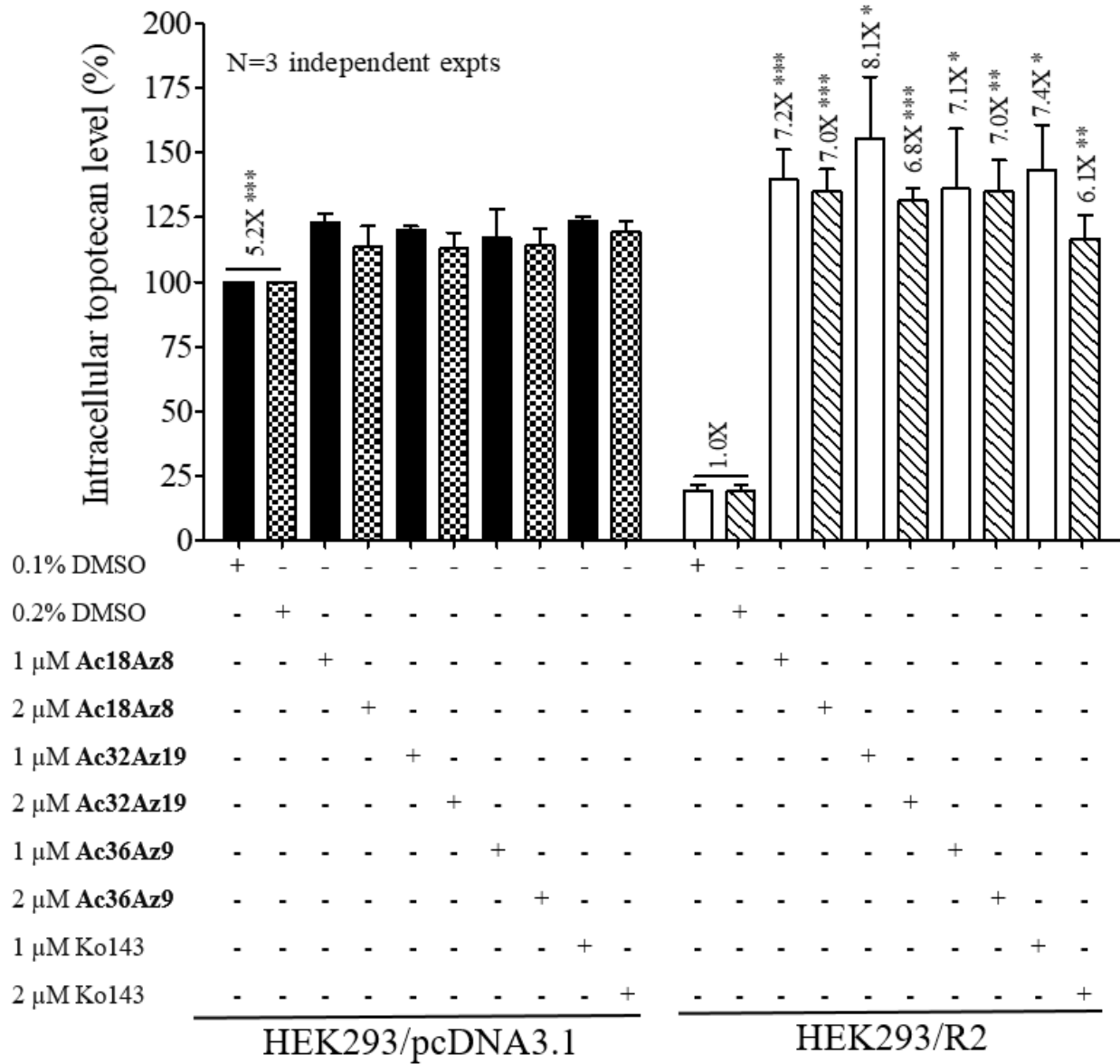
258 The above results show that these triazole-bridged flavonoids are potent, nontoxic and
 259 highly selective BCRP modulators (**Table 2** and **Table 3**). We determine whether the reversal of
 260 BCRP-mediated drug resistance is associated with an increase in drug accumulation. As shown in
 261 **Figure 4**, BCRP-overexpressing cell line HEK293/R2 significantly accumulates 5.2-fold
 262 (p<0.005) and 4.4-fold (p<0.005) less topotecan (**Figure 4A**) and mitoxantrone (**Figure 4B**) as
 263 compared to its wild type. In the presence of 1 or 2 μM of triazole-containing flavonoids or Ko143,
 264 intracellular topotecan and mitoxantrone levels are significantly increased and comparable to that
 265 observed for the non-BCRP parental cell line, HEK293/pcDN3.1 (**Figures 4A and 4B**). In contrast,

266 **Ac18Az8 Ac32Az19** and **Ac36Az9** do not affect the intracellular topotecan or mitoxantrone level
267 in wild type HEK293/pcDNA3.1 cells. The result suggests that these triazole-bridged flavonoids
268 inhibit transport activity of BCRP and increase drug retention inside the cells.

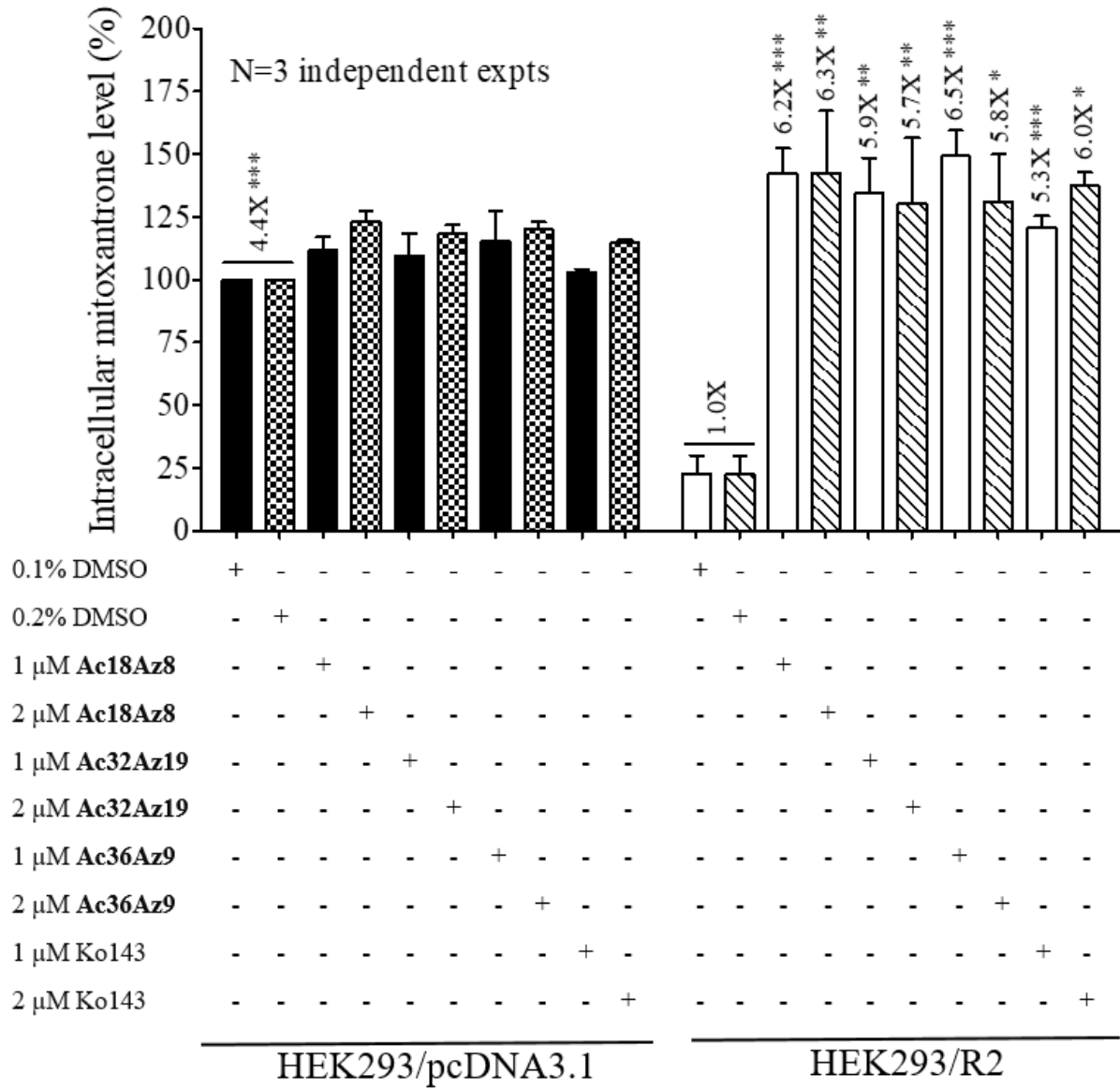
269 We investigate if the triazole-containing flavonoids could block BCRP-mediated drug efflux
270 in BCRP-overexpressing cells. Both wild type and HEK293/R2 cells are pre-loaded with
271 mitoxantrone, then the cells are transferred to drug-free media to allow mitoxantrone efflux.
272 Without **Ac32Az19**, the intracellular mitoxantrone level of HEK293/R2 cells significantly
273 decreases to 47% in 150 min ($p < 0.05$) (**Figure 4C**). In the presence of 2 μ M of **Ac32Az19**,
274 mitoxantrone efflux is dramatically inhibited. The intracellular mitoxantrone level remains at 94%
275 after 150 min (**Figure 4C**). With or without **Ac32Az19**, no observable change in the efflux rate is
276 noted in non-BCRP expressing wild type. The above result demonstrates that the reversal of drug
277 resistance by **Ac32Az19** in HEK293/R2 cells is due to the blockage of drug efflux, leading to an
278 increased drug accumulation and thus restoring the chemosensitivity of BCRP-overexpressing cell
279 line towards anticancer drugs again.

280 BCRP is an efflux transporter with broad substrate specificity. In order to study whether
281 **Ac32Az19** is itself a substrate of BCRP, its intracellular level is measured after treating the
282 HEK293/pcDNA3.1 or HEK293/R2 cells for 2 hr. At 2 or 10 μ M of **Ac32Az19** alone, intracellular
283 **Ac32Az19** levels in HEK293/R2 cells are the same as that in HEK293/pcDNA3.1 cells (**Figure**
284 **4D**), suggesting that **Ac32Az19** is not a transport substrate of BCRP.

(A)

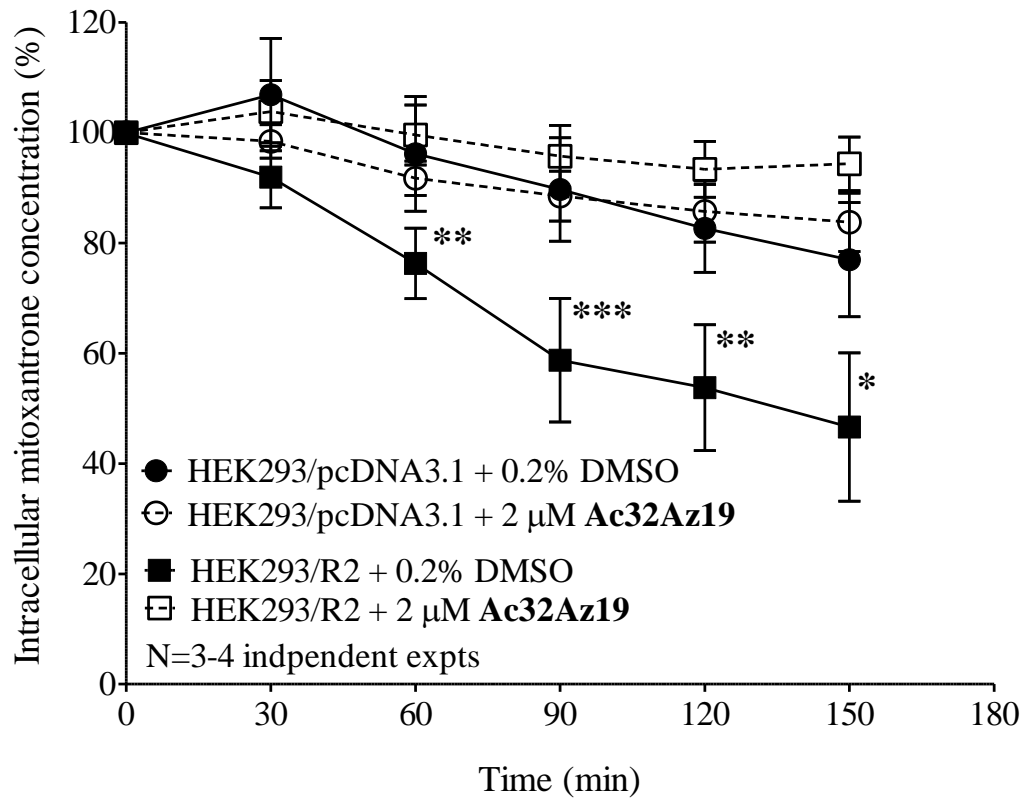


(B)

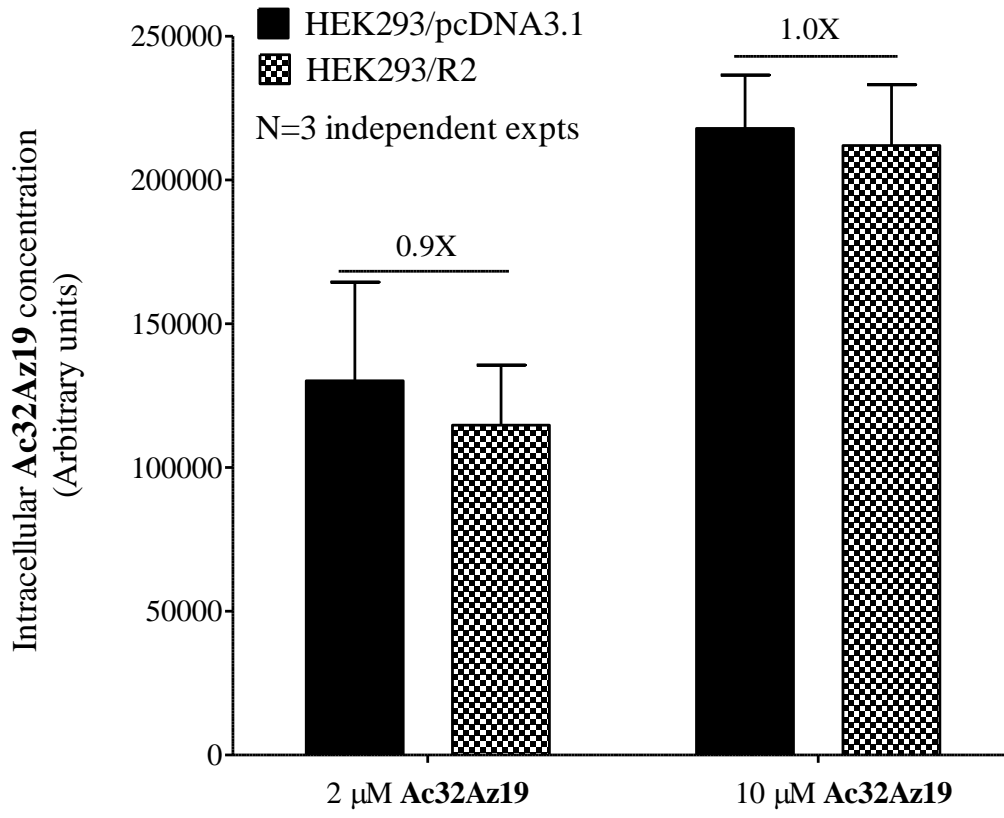


(C)

Mitoxantrone efflux



(D)



288

289

290 **Figure 4.** Effect of **Ac18Az8**, **Ac32Az19** and **Ac36Az9** on intracellular accumulation of BCRP-
291 drug substrates in HEK293/pcDNA3.1 and HEK293/R2 cells. HEK293/pcDNA3.1 or HEK293/R2
292 cells are co-incubated with 1 or 2 μ M of modulators and anticancer drugs (A) topotecan or (B)
293 mitoxantrone for 2 hr at 37 °C. Intracellular levels of drugs are measured by flow cytometer. The
294 intracellular level of drug after treatment is normalized to wild type HEK293/pcDNA3.1 cells. A
295 0.1 % or 0.2 % of DMSO is used as a negative control. Student paired t test is conducted relative
296 to HEK293/R2 cells incubated with 0.1 % or 0.2 % DMSO. * $p < 0.05$, ** $p < 0.01$ and *** $p < 0.005$.
297 (C) To measure mitoxantrone efflux, wild type and HEK293/R2 cells are pre-incubated in
298 supplemented RPMI1640 containing 5 μ M mitoxantrone for 1 hr at 37 °C. Then the cells are
299 washed and further incubated with or without 2 μ M **Ac32Az19**. At 0, 30, 60, 90, 120 and 150
300 min, the cells are harvested for measuring the intracellular mitoxantrone level using flow
301 cytometer at FL-4 channel. Student paired t test is conducted with or without **Ac32Az19** at
302 different time points in HEK293/R2 cells. * $p < 0.05$, ** $p < 0.01$ and *** $p < 0.005$. (D) To determine
303 intracellular **Ac32Az19** concentration, 1×10^7 cells are incubated with 2 or 10 μ M of **Ac32Az19**
304 at 37 °C for 2 hr. Cells are then washed with ice cold PBS. To the cell pellet, acetonitrile is added
305 to lyse the cells and the supernatant is saved for **Ac32Az19** determination using UPLC-MS/MS.
306 All values in **Figure 4** are presented as mean \pm standard error of mean.

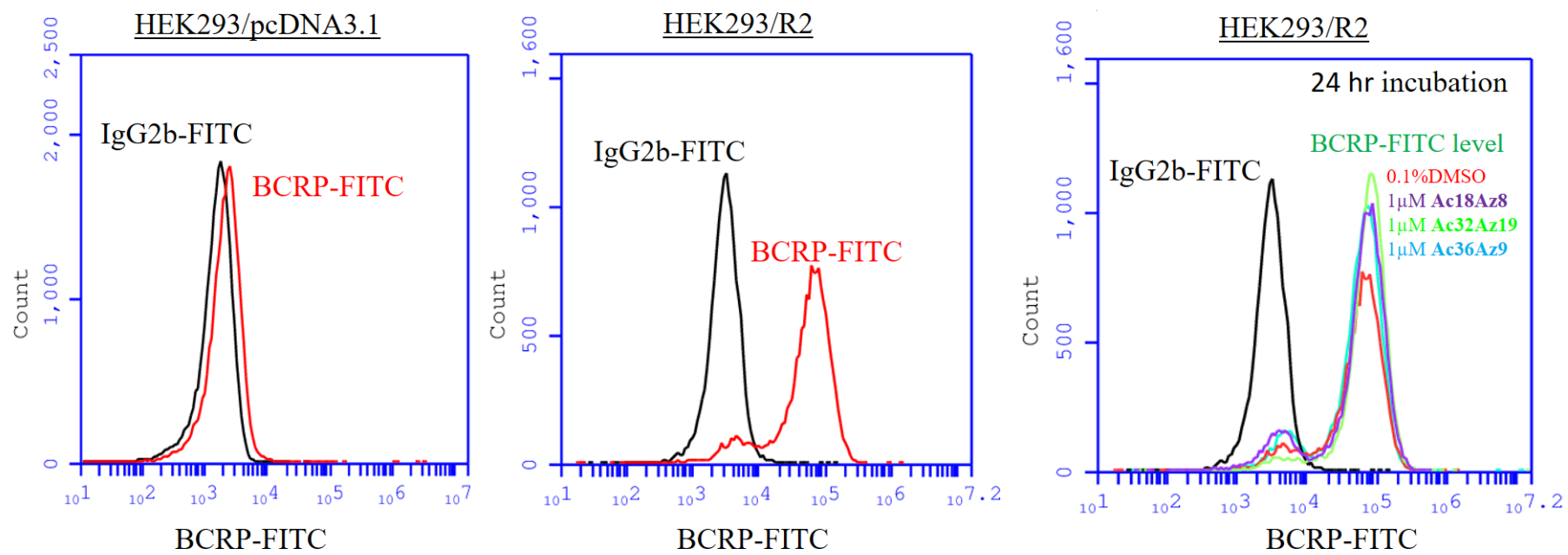
307 **2.2.5 BCRP inhibitors Ac18Az8, Ac32Az19 and Ac36Az9 do not affect BCRP protein expression**
308 levels in HEK293/R2 cells

309 MDR modulation in cancers can sometimes be due to lowered expression of the
310 transporter proteins and not to direct inhibition of pumping activity. We investigate if **Ac18Az8**,
311 **Ac32Az19** and **Ac36Az9** could affect BCRP level in HEK293/R2 cells. We characterize the effect
312 of these triazole-containing flavonoids on cell surface BCRP protein level by flow cytometry

313 **(Figure 5A)**. The cell surface BCRP protein level in HEK293/R2 cells is 91- to 110-fold higher
314 than the wild type HEK293/pcDNA3.1 **(Figure 5B)**. After incubating with 1 or 3 μ M of these
315 triazole-bridged flavonoids for 24 hr, cell surface BCRP protein level in HEK293/R2 cells is
316 slightly decreased or increased by -10 % to 30 %, indicating that they do not down-regulate the
317 cell surface BCRP protein level to chemosensitize the cells towards topotecan or mitoxantrone.
318 Therefore, the increased drug retention observed in BCRP-overexpressing HEK293/R2 cell line
319 after triazole-containing flavonoid treatment is not due to the reduction of cell surface BCRP
320 protein level, but due to the blockage of BCRP efflux activity.

321

(A)



(B)

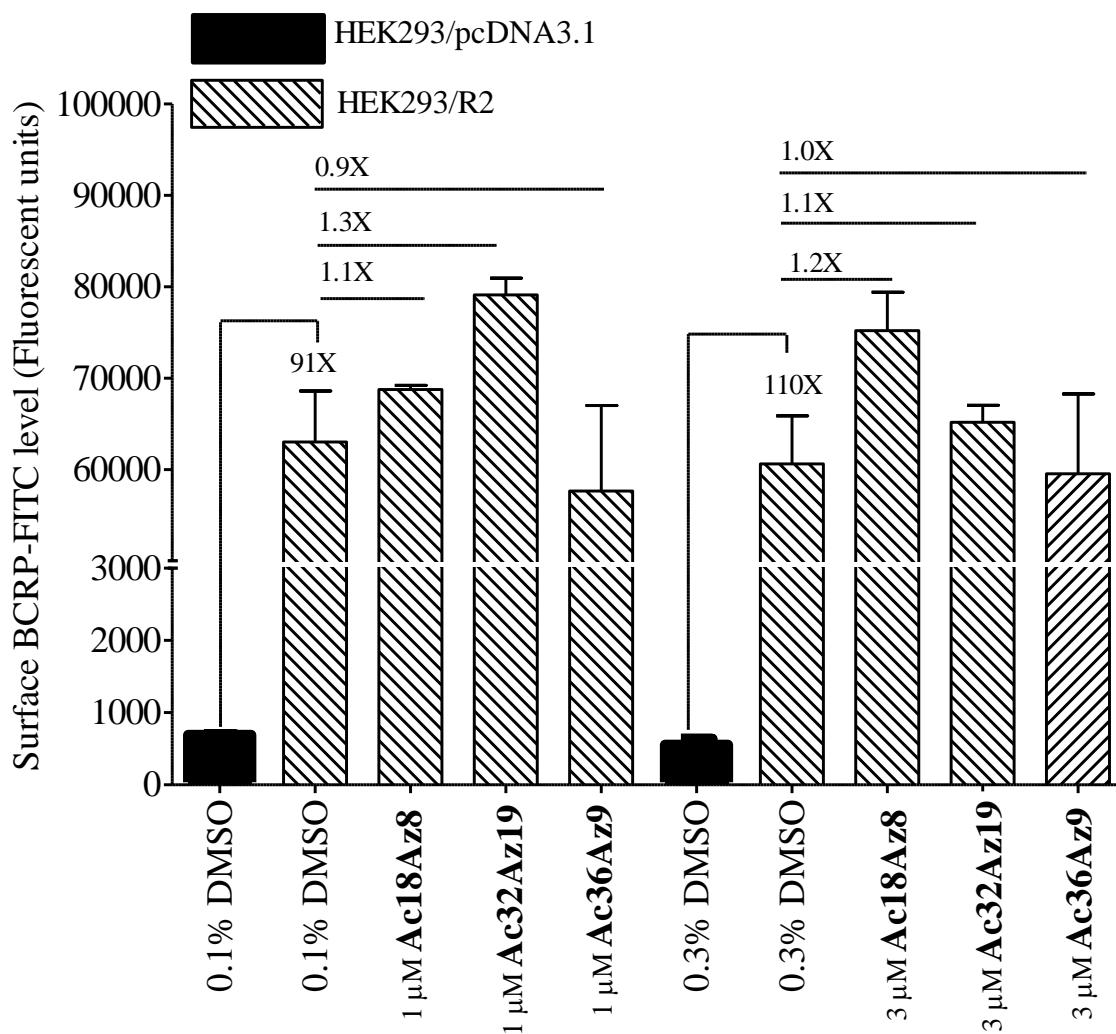


Figure 5. Effect of triazole-containing flavonoids on cell surface BCRP protein expression level. HEK293/pcDNA3.1 and HEK293/R2 cells are treated with or without 1 or 3 μM of triazole containing flavonoids for 24 hr. Cell surface BCRP protein level is measured by flow cytometer at FL1 channel. (A) The cell surface BCRP protein level in HEK293/pcDNA3.1 and HEK293/R2 cells is analyzed using BCRP-FITC antibody. IgG2b-FITC is an isotype control. (B) The surface BCRP protein level of HEK293/R2 cells is detected after incubating with 1 or 3 μM of tested compounds for 24 hr respectively. 0.1 % or 0.3 % of DMSO is used as a solvent control.

2.2.6 Ac32Az19 has weak effect on substrate stimulated BCRP-ATPase activity

In order to study if **Ac32Az19** could inhibit ATPase activity of BCRP and then block transporter efflux, microsome fraction from BCRP-overexpressing cell line S1M180 is purified and the effect of **Ac32Az19** on vanadate-sensitive BCRP-ATPase activity is investigated. In contrast to Ko143 which is a known inhibitor of BCRP-ATPase, it is found that **Ac32Az19** slightly increases vanadate-sensitive BCRP-ATPase activity from 110 % to 120 % when raising the concentration from log -1 to log 4 nM (**Figure 6**).

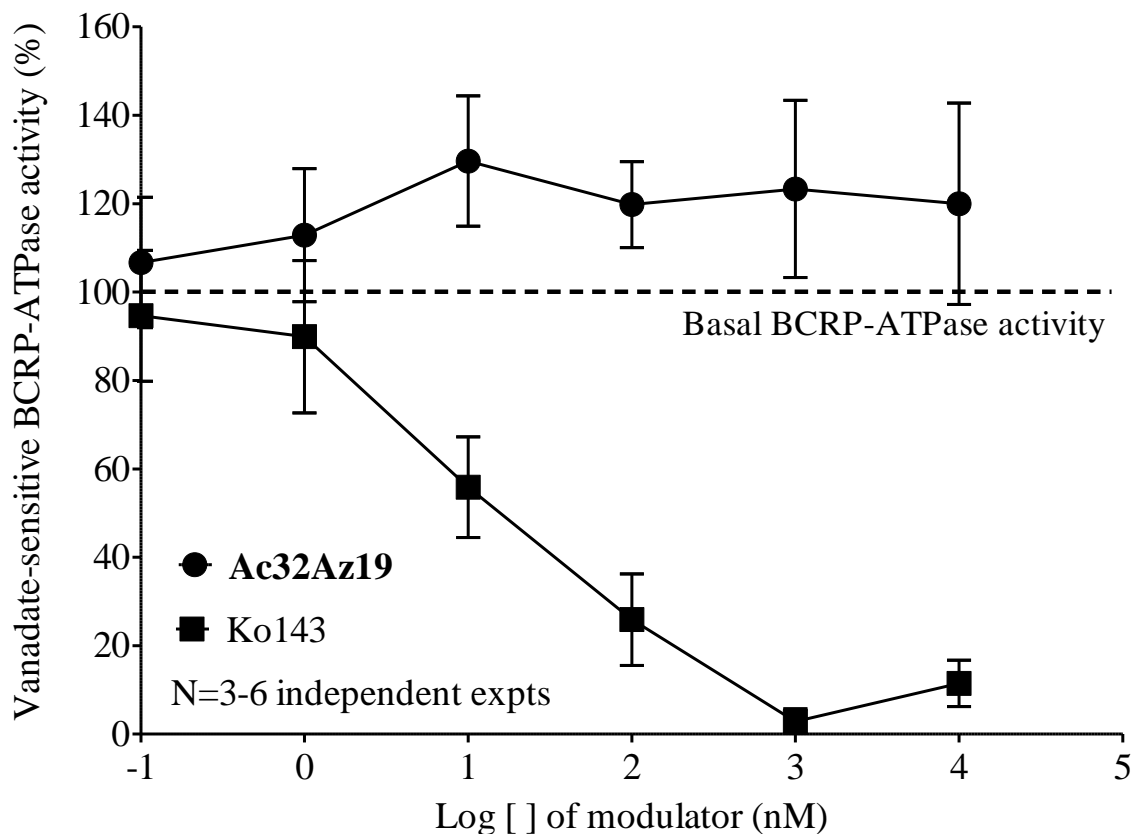


Figure 6. Effect of **Ac32Az19** on vanadate-sensitive BCRP-ATPase activity. S1M180 is a mitoxantrone selected colon cancer cell line and has BCRP overexpression. Membrane fraction of S1M180 is collected after sonication and ultracentrifugation. Ouabain (Na^+/K^+ -ATPase inhibitor)

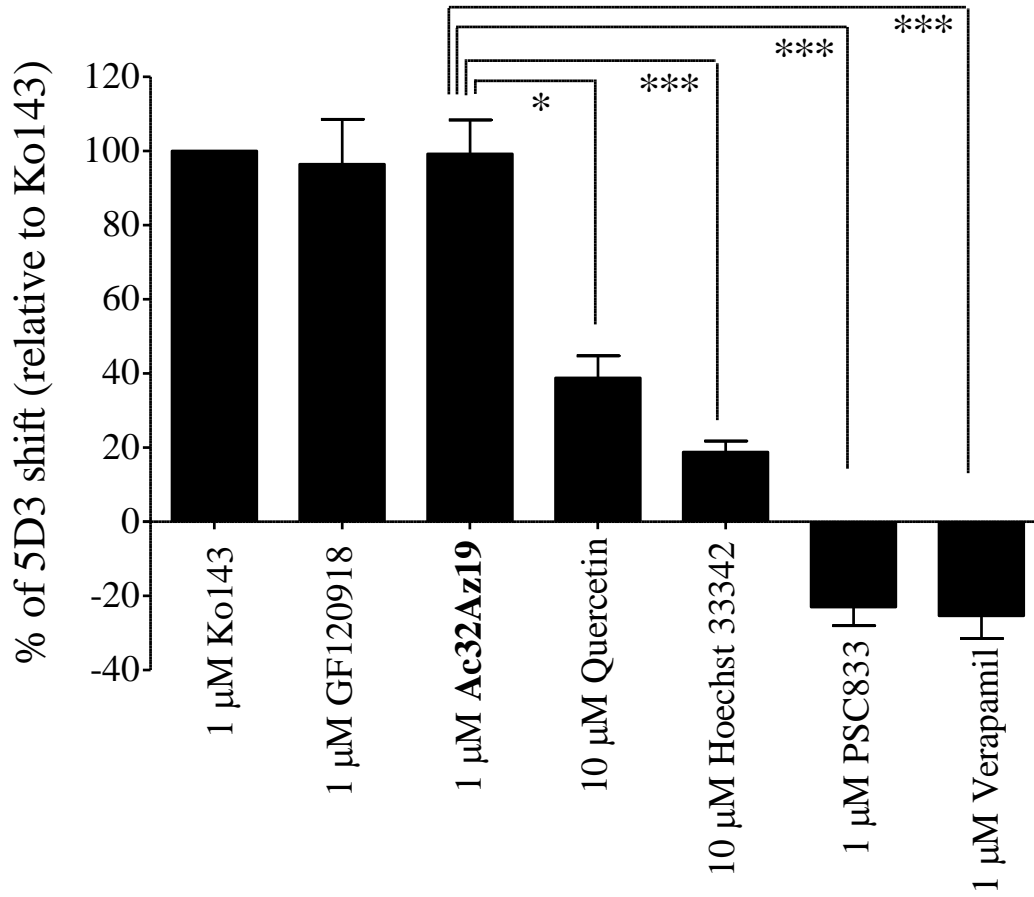
and sodium azide (F-type ATPase inhibitor) are added to the microsome fraction to inhibit non-ABC transporter ATPase activities. Sodium *orthovanadate* inhibits ABC transporter ATPase activity and is used to calculate vanadate-sensitive activity by subtraction from the total ATPase activity (without sodium *orthovanadate*). Ko143 and **Ac32Az19** are pre-incubated at 37 °C for 30 min, followed by 1 hr incubation of 2.5 mM ATP. After the reaction is stopped, phosphate level is determined using colorimetry method. These data are shown as mean \pm standard error of mean.

2.2.7 Effect of **Ac32Az19** on conformation of BCRP using 5D3 monoclonal antibody

5D3 is a conformation sensitive monoclonal antibody and can recognize extracellular CD338 epitope of the human BCRP. Its binding to BCRP (i.e. 5D3 shift) can be increased when BCRP substrates /inhibitors interacting with BCRP.⁶² Inhibitors of BCRP are reported to have higher 5D3 shift as compared to those caused by transported substrates.⁶³ Effect of **Ac32Az19** on conformational change of BCRP and 5D3 shift is studied using BCRP-overexpressing cell line HEK293/R2. Specific BCRP inhibitor Ko143 at 1 μ M is used as a positive control and set as a 100 % 5D3 shift relative to untreated DMSO control (**Figure 7A**). A histogram showing 5D3 shift caused by BCRP inhibitors/substrates or P-gp inhibitors (PSC833 and verapamil) is presented in **Figures 7B, 7C and 7D**. As remarkable as Ko143, **Ac32Az19** and another BCRP inhibitor GF120918 at 1 μ M also cause 100 % 5D3 shift, indicating that both of them can interact with BCRP and cause higher amount of conformational change of BCRP (**Figures 7A and 7B**). On the contrary, known BCRP substrates, quercetin and Hoechst 33342 even at 10 μ M are found to only slightly increase 5D3 shift, about 39 % and 19 % relative to Ko143 (**Figures 7A and 7C**). **Ac32Az19** causing higher 5D3 shift supports that it is not transport substrate but rather inhibitor

of BCRP. Specific P-gp inhibitors PSC833 and verapamil do not increase 5D3 shift (**Figures 7A** and **7D**), suggesting that they cannot interact with BCRP.

(A) N=3-6 independent expts



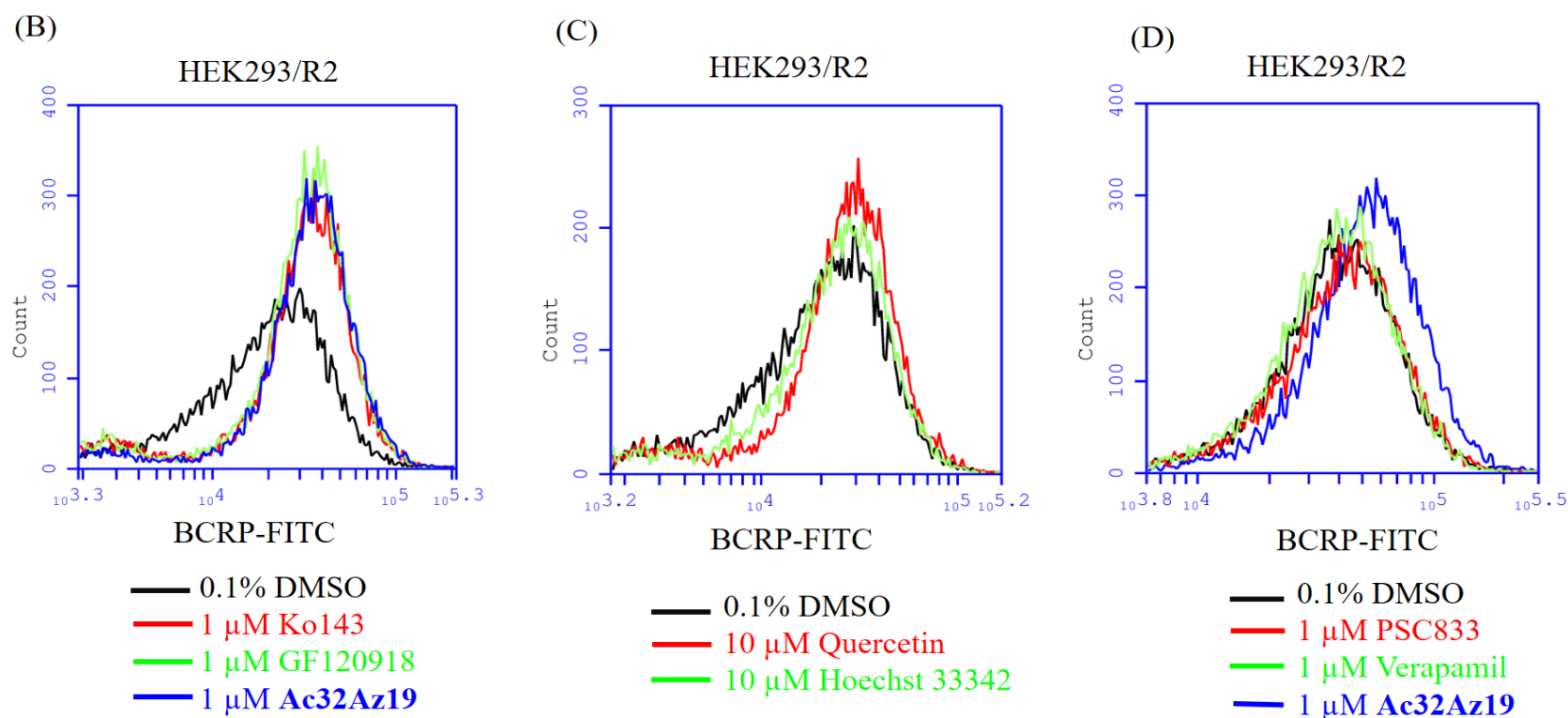


Figure 7. Effect of **Ac32Az19** on 5D3 labeling in HEK293/R2 cells. (A) % of 5D3 shift caused by **Ac32Az19**, known BCRP inhibitors/substrates and known P-gp inhibitors is compared. Ko143 at 1 μ M is used as a positive control and set as a 100 % 5D3 shift. Ko143 (1 μ M), GF120918 (1 μ M), **Ac32Az19** (1 μ M), quercetin (10 μ M), Hoechst 33342 (10 μ M), PSC833 (1 μ M) and verapamil (1 μ M) are present during BCRP-FITC antibody labeling. The values are presented as mean \pm standard error of mean. Student paired t test

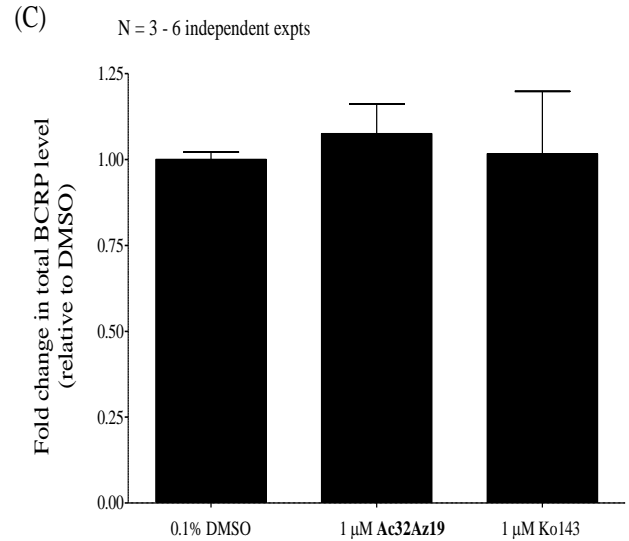
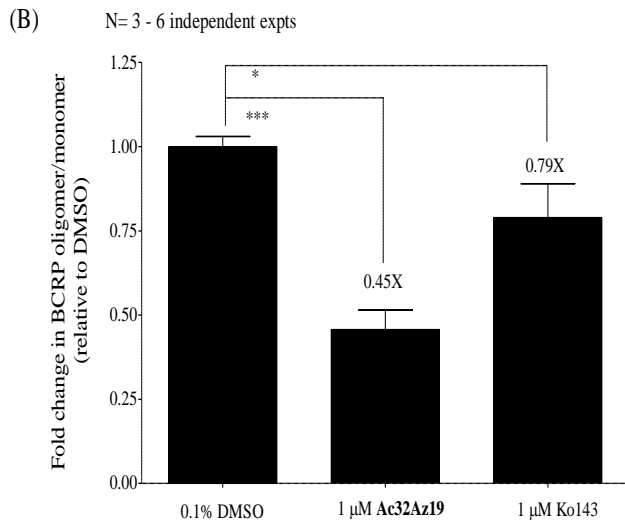
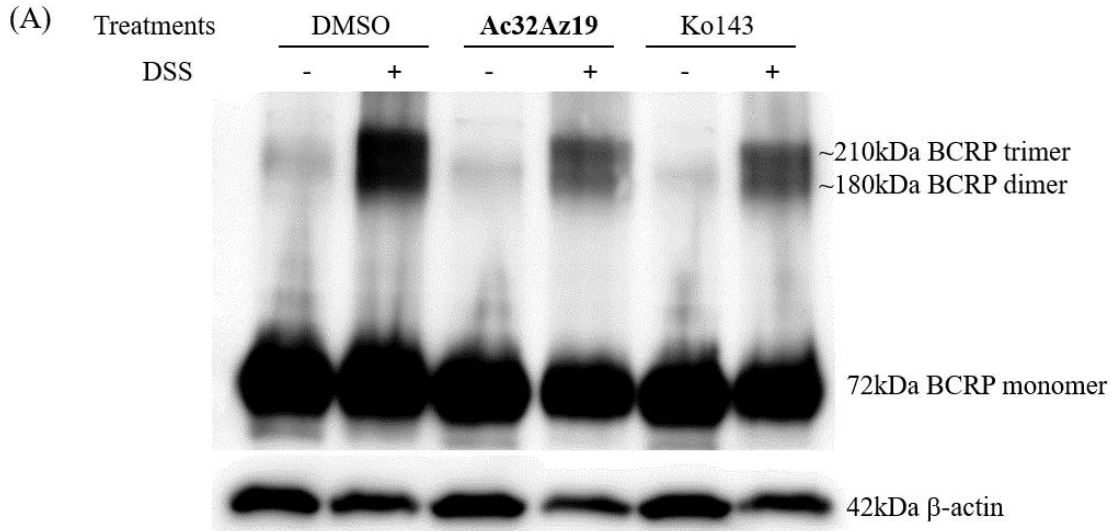
is conducted relative to **Ac32Az19**. * $p < 0.05$, ** $p < 0.01$ and *** $p < 0.005$. Representative 5D3 shift histogram caused by (B) BCRP specific inhibitors including Ko143, GF120918 and **Ac32Az19**, (C) BCRP substrates including quercetin and Hoechst 33342 and (D) P-gp inhibitors including PSC833 and verapamil and **Ac32Az19**.

2.2.8 Effect of **Ac32Az19** on the ratio of BCRP oligomer to monomer

BCRP is composed of one NBD and one TMD. A functional ABC transporter like P-gp and MRP1 requires two TMDs and two NBDs to form a central translocation pathway. It has been reported that the functional BCRP may exist as a homo-dimer or -oligomer for substrate binding and transport.⁶⁻⁸ We investigate if **Ac32Az19** could reduce the abundance of functional BCRP dimer or oligomer. HEK293/R2 cells are pre-treated with 1 μM of **Ac32Az19** for 4 days and then further incubated with or without chemical cross-linking reagent disuccinimidyl suberate (DSS) with an arm length of 11.4 Å. If BCRP dimer or oligomer exists, it can be cross-linked by DSS and can be separated and detected by the SDS-PAGE and Western blot.

As shown in **Figure 8A**, two bands of BCRP with protein size greater than that of BCRP monomer are clearly detected after DSS cross-linking when comparing to the control without DSS. Their sizes are around 210 kDa and 180 kDa which represent the trimeric and dimeric BCRP, respectively.⁶⁴ After treating with **Ac32Az19**, the abundance of dimer and trimer are obviously reduced (**Figure 8A**). When comparing to the untreated DMSO control, the ratio of oligomer to monomer is significantly decreased to 0.45- ($p < 0.005$) and 0.8-fold ($p < 0.05$) in **Ac32Az19** and Ko143 treated cells, respectively (**Figure 8B**). Similar to the flow cytometry data (**Figure 5B**), **Ac32Az19** does not affect the total BCRP protein level (**Figure 8C**). It has been demonstrated that dimeric or oligomeric BCRP is responsible for mitoxantrone transport and **Ac32Az19** treated cells

with half abundance of functional BCRP dimers/oligomers results in 3.8-fold ($p < 0.005$) more mitoxantrone accumulation than the untreated DMSO cells (**Figure 8D** and **8E**). On the contrary, Ko143-treated cells with 20% BCRP dimers/oligomers reduction results in 2-fold ($p < 0.05$) increase in mitoxantrone accumulation (**Figure 8D** and **8E**).



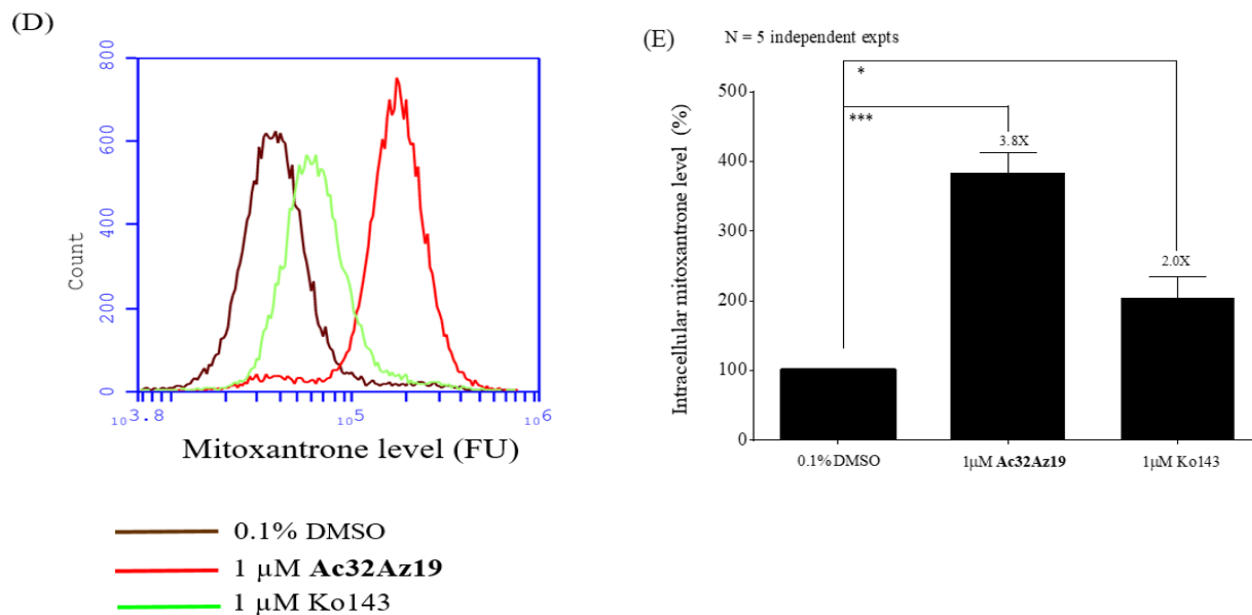


Figure 8. Effect of **Ac32Az19** on the ratio of BCRP oligomer to monomer. HEK293/R2 cells are pre-treated with **Ac32Az19** (1 μ M), Ko143 (1 μ M) and 0.1% DMSO for 4 days and then further incubated with or without chemical cross-linking reagent disuccinimidyl suberate (DSS) for 45 min. (A) 50 μ g of cell lysates from HEK293/R2 cells with or without cross-linking are separated on the SDS-PAGE and then Western blot analysis. (B) After cross-linking, the protein levels of BCRP monomer, dimer and trimer in the Western blot are analyzed by ImageJ software. The ratio of BCRP oligomer to monomer after each treatment = protein level of dimer and trimer / protein level of monomer. The fold-change in BCRP oligomer/monomer was relative to the solvent control 0.1 % DMSO. N = 3-6 independent experiments. (C) Without cross-linking, the protein levels of BCRP monomer and β -actin after each treatment are determined by ImageJ software. β -actin here is used as a loading control. The actual level of BCRP is normalized to β -actin level accordingly. The fold change in total BCRP level is relative to the solvent control 0.1 % DMSO. N = 3-6 independent experiments. (D) After 4-day treatment with modulator (1 μ M) at 37 $^{\circ}$ C with 5 % CO₂, the cells are harvested to perform mitoxantrone accumulation assay and its level is measured

by flow cytometry as described previously. Modulator-treated cells contain more mitoxantrone than the untreated DMSO cells. (E) The intracellular mitoxantrone level in each treatment group is relative to 0.1 % DMSO. N = 5 independent experiments. The values in this figure are presented as mean \pm standard error of mean. Student paired t test is conducted relative to 0.1% DMSO. *p < 0.05, **p < 0.01 and ***p < 0.005.

3. DISCUSSION AND CONCLUSION

Several clinical trials to overcome MDR by co-administration of an inhibitor of ABC transporters with an anti-cancer drug had led to disappointing outcomes.⁶⁵ Further improvement of inhibitors of ABC transporters should not only focus on potency but also on improving specificity to minimize potential drug-drug interaction as well as reducing toxicity.³⁴

In a 40-member flavonoid monomer library, we found that six of them displayed strong inhibition against BCRP with EC_{50} less than 100 nM (**Table 1**). **Ac32**, **Az8** and **Az9** with *m*-methoxycarbonylbenzyloxy substitution at C-3 of C-ring were found to be potent inhibitors with EC_{50} value in the range of 8.5 to 80.3 nM, nearly as active as Ko143 ($EC_{50} = 9$ nM) (**Table 1**). Subsequently, we chose **Ac32**, **Az8** and **Az9** monomers as the lead fragments and by employing the CuAAC reaction to form triazole-containing flavonoids. Three compounds, **Ac18Az8**, **Ac32Az19** and **Ac36Az9**, were found to be highly active BCRP specific inhibitor with $EC_{50} = 1 - 15$ nM for reversing topotecan resistance vs Ko143 = 9 nM, with high BCRP selectivity over P-gp and MRP1 (BCRP selectivity over P-gp > 67- 286 vs Ko143 = 118-122 and BCRP selectivity over MRP1 > 67 – 714 vs Ko143 = 217-224) and nontoxic (IC_{50} towards L929 > 100 μ M vs Ko143 = 31 μ M) (**Table 2**).

It was demonstrated that they inhibited the mitoxantrone efflux activity of BCRP (**Figure 4C**), thus elevated the intracellular drug accumulation (**Figure 4A and 4B**) and finally restored the drug sensitivity of the BCRP-overexpressing cells (**Tables 1 and 2**). On the other hand, **Ac32Az19** exhibited similar intracellular level in wild type and BCRP-overexpressing cell line HEK293/R2 (**Figure 4D**) suggesting that **Ac32Az19** is an inhibitor of BCRP, rather than a transport substrate of BCRP.

It is important to understand the possible mechanism by which these flavonoid monomers exert inhibition on BCRP. They did not down-regulate the surface BCRP protein expression, so that it could not be the mechanism to enhance the drug retention (**Figure 5**). In a previous investigation of various flavonoids as BCRP inhibitors, a SAR study of 25 flavonoids as BCRP inhibitors led to the suggestion that the inhibition may involve, in part, the binding of flavonoids with the NBD of BCRP.⁵⁰ One would expect that such a binding of flavonoid with the NBD of BCRP should lead to an inhibition of ATPase activity, inconsistent with the experimental observation that **Ac32Az19** did not inhibit BCRP-ATPase activity (**Figure 6**).

Recently, based on cryo-EM structures, a model of drug capture and extrusion by ABCG2 in the dimeric state has been proposed.⁵⁵ While **Ac32Az19** at 1 μ M caused 100 % 5D3 shift, indicating that it can interact with BCRP and cause conformational change of BCRP (**Figure 7**), **Ac32Az19** did not inhibit BCRP-ATPase activity whereas inhibitors such as Ko143 did (**Figure 6**) as expected from the proposed model.⁵⁵ The binding of **Ac32Az19** to the BCRP dimer does not satisfactorily account for its inhibitory activity.

Unlike dimeric P-gp and MRP1, BCRP is a 72 kDa half transporter and consists of one NBD and one TMD.⁵ BCRP forms a dimer or oligomer when it functions as a transporter.⁶⁻⁸ The dimer/oligomer could be formed by intermolecular covalent bond formation,⁶⁶ likely through cys630⁶⁷ or possibly even by non-covalent interaction.⁶⁸ One plausible approach to inhibit the function of BCRP is to inhibit its dimerization/oligomerization process. We found that **Ac32Az19** reduced the abundance of dimer and trimer (**Figure 8A**) when compared to the untreated DMSO control. The ratio of dimer/oligomer to monomer was significantly decreased to 0.45-fold ($p < 0.005$) in **Ac32Az19** treated cells (**Figure 8B**). Similar to the flow cytometry data (**Figure 5B**), **Ac32Az19** did not affect the total BCRP protein level (**Figure 8C**). A greater than 50% reduction in the

abundance of BCRP dimer/oligomer led to 3.8-fold ($p < 0.005$) more mitoxantrone accumulation in **Ac32Az19** treated cell (**Figure 8D** and **8E**). At this time, we do not know the exact nature of the inhibition, whether it is by disrupting the covalent disulfide bond formation or simply the non-covalent interaction. By inhibiting BCRP dimerization or oligomerization, it offers a promising strategy to reverse BCRP-mediated MDR. This may also explain the observation that **Ac32Az19** has higher BCRP selectivity against P-gp and MRP1 due to the structural difference among ABC transporters. Both P-gp and MRP1 are homodimers, whereas the BCRP is a monomer and can only function as a transporter when it forms dimer or oligomer. (**Tables 2** and **3**).

The flavonoid monomers **Ac18Az8**, **Ac32Az19** and **Ac36Az9** are nearly half the size of the dimer (MW of monomer = 674 - 748 vs **Ac22(Az8)₂** = 1230), have lower cLogP value (cLogP of monomer = 5.10 - 6.64 vs **Ac22(Az8)₂** = 10.46) and tPSA value (tPSA value of monomer = 99.02 - 140.95 vs **Ac22(Az8)₂** = 216.50). The smaller monomers are likely to have better permeability and druggability than the dimer. All in all, monomeric triazole-containing flavonoids have the potential to be developed into combination therapy to overcome MDR in cancers with BCRP overexpression.

4. EXPERIMENTAL SECTION

4.1. Chemistry

All NMR spectra were recorded on a Bruker Advance-III 400 MHz spectrometer at 400 MHz for ^1H and 101 MHz for ^{13}C , Varian Unity Inova 500 MHz NMR Spectrometer at 500 MHz for ^1H and 126 MHz for ^{13}C or Bruker Advance-III 600 MHz spectrometer at 600 MHz for ^1H and 151 MHz for ^{13}C . All NMR measurements were carried out at room temperature and the chemical shifts are reported as parts per million (ppm) in unit relative to the resonance of CDCl_3 (7.26 ppm in the ^1H , 77.0 ppm for the central line of the triplet in the ^{13}C modes, respectively). Low-resolution and high-resolution mass spectra were obtained on a Micromass Q-TOF-2 by electron spray ionization (ESI) mode or on Finnigan MAT95 ST by electron ionization (EI) mode. All reagents and solvents were reagent grade and were used without further purification unless otherwise stated. The plates used for thin-layer chromatography (TLC) were E. Merck Silica Gel 60F₂₅₄ (0.25 mm thickness) and they were visualized under short (254 nm) and long (365 nm) UV light. Chromatographic purifications were carried out using MN silica gel 60 (230 – 400 mesh). The purity of tested compounds was determined by HPLC, which was performed by using Agilent 1100 series installed with an analytic column of Agilent Prep-Sil Scalar column (4.6 mm x 250 mm, 5 μm) at UV detection of 320 nm (reference at 450 nm) with isocratic elution of hexane (50 %)/ethyl acetate (25 %)/methanol (25 %) at a flow rate of 1.0 mL/min. All tested compounds were shown to have >95 % purity according to HPLC.

The synthesis of 30 monomers have been reported previously including **Ac1-Ac13**, **Ac16**, **Ac33**, **Ac35**, **Ac42**, **Az1-Az3**, **Az5**, **Az7-Az13**, **Az17** and **Az18**.^{56, 57}

4.1.1 Synthesis of 2-(4-(Pent-4-yn-1-yloxy)phenyl)-4H-chromen-4-one (Ac1): This compound was obtained according to the procedure as described.⁵⁶

4.1.2 Synthesis of 7-(Pent-4-yn-1-yloxy)-2-phenyl-4H-chromen-4-one (Ac2): This compound was obtained according to the procedure as described.⁵⁶

4.1.3 Synthesis of 7-Fluoro-2-(4-(pent-4-yn-1-yloxy)phenyl)-4H-chromen-4-one (Ac3): This compound was obtained according to the procedure as described.⁵⁶

4.1.4 Synthesis of 5-(Benzyloxy)-7-(methoxymethoxy)-2-(4-(pent-4-yn-1-yloxy)phenyl)-4H-chromen-4-one (Ac4): This compound was obtained according to the procedure as described.⁵⁶

4.1.5 Synthesis of 2-(4-(Hex-5-yn-1-yloxy)phenyl)-6-methyl-4H-chromen-4-one (Ac5): This compound was obtained according to the procedure as described.⁵⁶

4.1.6 Synthesis of (E)-3-(4-(Hex-5-yn-1-yloxy)phenyl)-1-(2-hydroxyphenyl)prop-2-en-1-one (Ac6): This compound was obtained according to the procedure as described.⁵⁶

4.1.7 Synthesis of (E)-1-(5-Ethyl-2-hydroxyphenyl)-3-(4-(hex-5-yn-1-yloxy)phenyl)prop-2-en-1-one (Ac7): This compound was obtained according to the procedure as described.⁵⁶

4.1.8 Synthesis of (E)-3-(4-(Hex-5-yn-1-yloxy)phenyl)-1-(2-hydroxy-5-methylphenyl)prop-2-en-1-one (Ac8): This compound was obtained according to the procedure as described.⁵⁶

4.1.9 Synthesis of (E)-3-(4-(Hex-5-yn-1-yloxy)phenyl)-1-(2-hydroxy-4-methylphenyl)prop-2-en-1-one (Ac9): This compound was obtained according to the procedure as described.⁵⁶

4.1.10 Synthesis of (E)-1-(4-Fluoro-2-hydroxyphenyl)-3-(4-(hex-5-yn-1-yloxy)phenyl)prop-2-en-1-one (Ac10): This compound was obtained according to the procedure as described.⁵⁶

4.1.11 Synthesis of 2-(4-(Pent-4-yn-1-yloxy)phenyl)quinazolin-4(3H)-one (Ac11): This compound was obtained according to the procedure as described.⁵⁶

4.1.12 Synthesis of 7-(Hex-5-yn-1-yloxy)-2-phenyl-4H-chromen-4-one (Ac12): This compound was obtained according to the procedure as described.⁵⁶

4.1.13 Synthesis of 2-Phenyl-7-(2-(prop-2-yn-1-yloxy)ethoxy)-4H-chromen-4-one (Ac13): This compound was obtained according to the procedure as described.⁵⁶

4.1.14 Synthesis of 7-(2-(Benzyl(prop-2-yn-1-yl)amino)ethoxy)-2-phenyl-4H-chromen-4-one (Ac16): This compound was obtained according to the procedure as described.⁵⁶

4.1.15 Synthesis of tri(prop-2-yn-1-yl)amine (Ac17): This compound was commercially available.

4.1.16 Synthesis of N-benzyl-N-methylprop-2-yn-1-amine (Ac18): This compound was commercially available.

4.1.17 Synthesis of 2-(but-3-yn-1-yl)isoindoline-1,3-dione (Ac19): This compound was commercially available.

4.1.18 Synthesis of N,N-dibenzylprop-2-yn-1-amine (Ac20): This compound was commercially available.

4.1.19 Synthesis of N-(prop-2-yn-1-yl)aniline (Ac27): This compound was commercially available.

4.1.20 Synthesis of methyl 3-(((2-(4-(hex-5-yn-1-yloxy)phenyl)-4-oxo-4H-chromen-3-yl)oxy)methyl)benzoate (Ac32): To a well stirred solution of **Ac6** (2 mmol, 640 mg) in acetone (30 mL) was added H₂O₂ (1 equiv) and KOH (1.1 equiv). The reaction mixture was further refluxed for 6 hr. When TLC indicated complete consumption of starting material, the reaction mixture was poured into a beaker containing water at ice-bath temperature. The white precipitate formed was

collected by suction filtration. The white solid was washed with n-hexane and subjected to crystallization from MeOH to afford the desired compound **1b** (420 mg, 63 %). A round bottom flask was charged with **1b** (1 mmol, 340 mg), methyl 3-(bromomethyl)benzoate (1.1 mmol, 250 mg), K₂CO₃ (1.2 equiv) and acetone (20 mL). The reaction mixture was stirred at refluxing temperature for 12 hr. When TLC indicated complete consumption of starting material, solvent was rotary evaporated to dryness. Purification was performed by flash column chromatography on silica gel with acetone in DCM as eluent to furnish the desired compound **Ac32** (350 mg, 72 %). ¹H NMR (500 MHz, CDCl₃) δ 1.72 - 1.81 (m, 2 H), 1.97 (dd, *J* = 8.54, 6.59 Hz, 2 H), 2.00 (t, *J* = 2.68 Hz, 1 H), 2.32 (td, *J* = 6.95, 2.68 Hz, 2 H), 3.90 (s, 3 H), 4.08 (t, *J* = 6.34 Hz, 2 H), 5.16 (s, 2 H), 6.92 - 6.99 (m, 2 H), 7.36 (t, *J* = 7.81 Hz, 1 H), 7.42 (ddd, *J* = 8.05, 7.08, 0.98 Hz, 1 H), 7.50 - 7.55 (m, 1 H), 7.59 - 7.64 (m, 1 H), 7.66 - 7.71 (m, 1 H), 7.91 - 7.97 (m, 1 H), 7.97 - 8.03 (m, 3 H), 8.30 (dd, *J* = 8.30, 1.46 Hz, 1 H); ¹³C NMR (126 MHz, CDCl₃) δ 18.0, 24.9, 28.0, 51.9, 67.3, 68.7, 73.2, 83.8, 114.1, 117.8, 122.9, 124.0, 124.5, 125.5, 128.1, 129.1, 129.7, 130.0, 130.4, 133.1, 133.1, 137.1, 138.9, 155.0, 156.4, 160.8, 166.6, 174.7; LRMS (ESI) *m/z* 483 [M+H]⁺; HRMS (ESI) calcd for C₃₀H₂₇O₆ [M+H]⁺ 483.1820, found 483.1808.

4.1.21 Synthesis of 4-(hex-5-yn-1-yloxy)benzaldehyde (Ac33): This compound was obtained according to the procedure as described.⁵⁶

4.1.22 Synthesis of 2-(4-(hex-5-yn-1-yloxy)phenyl)-3-((3-methoxybenzyl)oxy)-4H-chromen-4-one (Ac35): This compound was obtained according to the procedure as described.⁵⁶

4.1.23 Synthesis of 2-(benzyl(prop-2-yn-1-yl)amino)ethanol (Ac36): This compound was commercially available.

4.1.24 Synthesis of 6-Fluoro-2-(4-(hex-5-yn-1-yloxy)phenyl)-4H-chromen-4-one (Ac41): A round bottom flask was charged with corresponding 4'-hydroxyflavone **2a** (2 mmol, 512 mg), 6-chlorohex-1-yne **2b** (2.4 mmol, 280 mg), K₂CO₃ (3 mmol, 414 mg), KI (0.2 mmol, 33 mg) and DMF (6 mL). The reaction mixture was stirred at refluxing temperature for 2 hr. When TLC indicated complete consumption of starting material, the reaction mixture was poured into a separating funnel containing water. The mixture was continuously extracted with DCM. If the mixture could not be separated into two layers, a small amount of 1 M HCl was added. The combined organic layers were dried over MgSO₄, filtered, and evaporated to give a brown crude reaction mixture. Purification was performed by flash column chromatography on silica gel with acetone in DCM as eluent to furnish desired product (0.57 g, 85 %). ¹H NMR (400 MHz, CDCl₃) δ 7.77 (dd, *J* = 8.5, 3.4 Hz, 3H), 7.48 (dd, *J* = 9.1, 4.1 Hz, 1H), 7.38 – 7.30 (m, 1H), 6.93 (d, *J* = 8.9 Hz, 2H), 6.64 (s, 1H), 4.01 (t, *J* = 6.3 Hz, 2H), 2.28 (td, *J* = 7.0, 2.6 Hz, 2H), 1.99 (t, *J* = 2.6 Hz, 1H), 1.96 – 1.89 (m, 2H), 1.76 – 1.68 (m, 2H). ¹³C NMR (101 MHz, CDCl₃) δ 18.1, 24.9, 28.1, 67.6, 68.9, 83.9, 105.5, 110.6 (d, *J*_{CF} = 23.5 Hz, C5), 115.2, 119.9 (d, *J*_{CF} = 8.1 Hz, C10), 121.7 (d, *J*_{CF} = 25.2 Hz, C7), 123.8, 125.1 (d, *J*_{CF} = 7.4 Hz, C8), 128.0, 152.3, 159.5 (d, *J*_{CF} = 245.1 Hz, C6), 162.0, 163.6, 177.3; LRMS (ESI) *m/z* 336.1 base peak: 336.1 [M+H]⁺; HRMS (ESI) calcd for C₂₁H₁₇FO₃ [M+H]⁺ 336.1161, found 336.1162.

4.1.25 Synthesis of 6-Fluoro-2-(4-(pent-4-yn-1-yloxy)phenyl)-4H-chromen-4-one (Ac42): This compound was obtained according to the procedure as described.⁵⁶

4.1.26 Synthesis of 7-(2-(benzylamino)ethoxy)-2-phenyl-4H-chromen-4-one (Ac43): The starting material 7-hydroxyflavone was prepared according to the procedure as described. To a well stirred solution of 7-hydroxyflavone **3a** (2.9 mmol, 0.7 g), *tert*-butyl benzyl(2-

hydroxyethyl)carbamate **3b** (2.9 mmol, 0.7 g) and PPh₃ (0.77 g, 1 equiv.) in THF (10 mL) at room temperature, was added DIAD (0.58 mL, 1 equiv.) dropwise. The reaction mixture was then stirred at refluxing temperature for 12 hr. The reaction mixture was evaporated to give a brown crude reaction mixture. Purification was performed by flash column chromatography on silica gel with hexane in ethyl acetate (1:10) as eluent to furnish *N*-Boc protected flavonoid compound (0.84 g, 70 %). A round-bottom flask was charged with *N*-Boc protected flavonoid compound (1.5 mmol, 0.7 g) and DCM (5 ml). The solution was cooled to 0 °C using an ice bath. An equal volume of TFA (5 mL) was then added dropwise, and the reaction mixture was stirred vigorously at 0 °C for 1 hr and at room temperature for another 3 hr. After the mixture was stirred, the reaction was quenched by pouring the mixture into a conical flask containing water. The resultant mixture was basified to pH 10 by using potassium hydroxide solution. The mixture was continuously extracted with DCM. The combined organic layers were dried over MgSO₄, filtered, and evaporated to give the desired product (0.5 g, 90%). ¹H NMR (400 MHz, CDCl₃) δ 2.05 (br. s., 1 H), 3.06 (t, *J* = 4.89 Hz, 2 H), 3.88 (s, 2 H), 4.17 (t, *J* = 4.89 Hz, 2 H), 6.72 (d, *J* = 1.96 Hz, 1 H), 6.89 - 6.99 (m, 2 H), 7.22 - 7.28 (m, 1 H), 7.29 - 7.39 (m, 4 H), 7.43 - 7.54 (m, 3 H), 7.85 (dd, *J* = 5.14, 1.96 Hz, 2 H), 8.09 (d, *J* = 8.56 Hz, 1 H); ¹³C NMR (101 MHz, CDCl₃) δ 47.6, 53.6, 68.1, 100.8, 107.2, 114.5, 117.7, 125.9, 126.8, 126.9, 127.9, 128.3, 128.8, 131.2, 131.6, 139.7, 157.7, 162.8, 163.2, 177.6; LRMS (ESI) *m/z* 372.2 base peak: 372.2 [M+H]⁺; HRMS (ESI) calcd for C₂₄H₂₂NO₃ [M+H]⁺ 372.1600, found 372.1602.

4.1.27 Synthesis of 2-(4-(2-(2-Azidoethoxy)ethoxy)phenyl)-4H-chromen-4-one (Az1): This compound was obtained according to the procedure as described.⁵⁶

4.1.28 Synthesis of 2-(4-(2-(2-(2-Azidoethoxy)ethoxy)ethoxy)phenyl)-4H-chromen-4-one (Az2):

This compound was obtained according to the procedure as described.⁵⁶

4.1.29 Synthesis of 2-(4-(2-(2-(2-Azidoethoxy)ethoxy)ethoxy)phenyl)-6-methyl-4H-chromen-4-one (Az3): This compound was obtained according to the procedure as described.⁵⁶

4.1.30 Synthesis of 2-(4-(2-(2-(2-Azidoethoxy)ethoxy)ethoxy)phenyl)-3-(benzyloxy)-4H-chromen-4-one (Az5): This compound was obtained according to the procedure as described.⁵⁶

4.1.31 Synthesis of 2-(4-(2-(2-Azidoethoxy)ethoxy)phenyl)-6-fluoro-4H-chromen-4-one (Az7): This compound was obtained according to the procedure as described.⁵⁶

4.1.32 Synthesis of methyl 3-(((2-(4-(2-(2-azidoethoxy)ethoxy)phenyl)-4-oxo-4H-chromen-3-yl)oxy)methyl)benzoate (Az8): This compound was obtained according to the procedure as described.⁵⁷

4.1.33 Synthesis of methyl 3-(((2-(4-(2-(2-(2-azidoethoxy)ethoxy)ethoxy)phenyl)-4-oxo-4H-chromen-3-yl)oxy)methyl)benzoate (Az9): This compound was obtained according to the procedure as described.⁵⁷

4.1.34 Synthesis of 2-(4-(2-(2-Azidoethoxy)ethoxy)phenyl)-3-(benzyloxy)-4H-chromen-4-one (Az10): This compound was obtained according to the procedure as described.⁵⁶

4.1.35 Synthesis of 7-(2-(2-Azidoethoxy)ethoxy)-2-phenyl-4H-chromen-4-one (Az11): This compound was obtained according to the procedure as described.⁵⁶

4.1.36 Synthesis of 7-(2-(2-(2-Azidoethoxy)ethoxy)ethoxy)-2-phenyl-4H-chromen-4-one (Az12): This compound was obtained according to the procedure as described.⁵⁶

4.1.37 Synthesis of 7-(2-Azidoethoxy)-2-phenyl-4H-chromen-4-one (Az13): This compound was obtained according to the procedure as described.⁵⁶

4.1.38 Synthesis of 2-(2-azidoethoxy)ethanol (Az16): This compound was commercially available.

4.1.39 Synthesis of 2-(4-(2-(2-azidoethoxy)ethoxy)phenyl)-3-((3-methoxybenzyl)oxy)-4H-chromen-4-one (Az17): This compound was obtained according to the procedure as described.⁵⁶

4.1.40 Synthesis of 2-(3-(2-(2-azidoethoxy)ethoxy)phenyl)-3-(benzyloxy)-4H-chromen-4-one (Az18): This compound was obtained according to the procedure as described.⁵⁶

4.1.41 Synthesis of (azidomethyl)benzene (Az19): This compound was commercially available.

4.2 General procedure for the synthesis of anti-triazole bridged flavonoid monomers catalyzed by Cu(I)

The Cu(PPh₃)₃Br catalyst (MW = 929) (0.05 mmol), prepared according to literature,⁶⁹ was added to a THF solution (2 mL) containing the azide (0.1 mmol) and the alkyne (0.1 mmol). The reaction mixture was stirred overnight under reflux condition. The crude residue was purified by flash chromatography on silica gel using gradient of 10 - 50 % of acetone with DCM to afford the desired compounds.

4.2.1 Synthesis of methyl 3-(((2-(4-(2-(2-(4-((benzyl(methyl)amino)methyl)-1H-1,2,3-triazol-1-yl)ethoxy)ethoxy)phenyl)-4-oxo-4H-chromen-3-yl)oxy)methyl)benzoate (Ac18Az8): This compound (41.8 mg) was obtained from **Ac18** and **Az8** in 62 % yield according to the general procedure described above. ¹H NMR (500 MHz, CDCl₃) δ 2.23 (s, 3 H), 3.55 (s, 2 H), 3.73 (s, 2 H), 3.82 - 3.86 (m, 2 H), 3.88 (s, 3 H), 3.98 (t, *J* = 5.12 Hz, 2 H), 4.12 - 4.17 (m, 2 H), 4.58 (t, *J* =

5.12 Hz, 2 H), 5.15 (s, 2 H), 6.94 (d, $J = 8.79$ Hz, 2 H), 7.18 - 7.24 (m, 1 H), 7.24 - 7.37 (m, 5 H), 7.42 (t, $J = 7.32$ Hz, 1 H), 7.51 (d, $J = 8.30$ Hz, 1 H), 7.60 (d, $J = 7.32$ Hz, 1 H), 7.65 - 7.71 (m, 2 H), 7.93 (d, $J = 7.81$ Hz, 1 H), 7.95 - 8.01 (m, 3 H), 8.29 (d, $J = 8.30$ Hz, 1 H); ^{13}C NMR (126 MHz, CDCl_3) δ 42.0, 50.2, 52.0, 52.1, 61.3, 67.3, 69.6, 69.8, 73.3, 114.3, 117.9, 123.6, 123.7, 124.2, 124.7, 125.8, 127.0, 128.2, 128.3, 129.0, 129.3, 129.8, 130.1, 130.5, 133.2, 133.3, 137.2, 139.1, 155.2, 156.3, 160.4, 166.8, 174.8; LRMS (ESI) m/z 675 $[\text{M}+\text{H}]^+$; HRMS (ESI) calcd for $\text{C}_{39}\text{H}_{39}\text{N}_4\text{O}_7$ $[\text{M}+\text{H}]^+$ 675.2819, found 675.2811.

4.2.2 Synthesis of *methyl 3-(((2-(4-(2-(2-(2-(4-((benzyl(methyl)amino)methyl)-1H-1,2,3-triazol-1-yl)ethoxy)ethoxy)ethoxy)phenyl)-4-oxo-4H-chromen-3-yl)oxy)methyl)benzoate* (**Ac18Az9**):

This compound (53.9 mg) was obtained from **Ac18** and **Az9** in 80 % yield according to the general procedure described above. ^1H NMR (500 MHz, CDCl_3) δ 2.23 (br. s., 2 H), 3.55 (br. s., 2 H), 3.60 - 3.76 (m, 7 H), 3.84 (t, $J = 4.64$ Hz, 2 H), 3.87 - 3.93 (m, 5 H), 4.17 (t, $J = 4.64$ Hz, 2 H), 4.55 (br. s., 2 H), 5.15 (s, 2 H), 6.95 (d, $J = 8.79$ Hz, 2 H), 7.23 (d, $J = 6.34$ Hz, 1 H), 7.27 - 7.38 (m, 5 H), 7.41 (t, $J = 7.57$ Hz, 1 H), 7.51 (d, $J = 8.30$ Hz, 1 H), 7.59 (d, $J = 7.81$ Hz, 1 H), 7.64 - 7.70 (m, 2 H), 7.93 (d, $J = 7.81$ Hz, 1 H), 7.98 (d, $J = 8.79$ Hz, 3 H), 8.26 - 8.31 (m, 1 H); ^{13}C NMR (126 MHz, CDCl_3) δ 42.1, 50.2, 52.0, 52.1, 61.3, 67.5, 69.6, 70.6, 70.7, 73.3, 114.4, 117.9, 123.4, 123.7, 124.2, 124.7, 125.8, 127.1, 128.2, 128.3, 129.0, 129.3, 129.8, 130.1, 130.5, 133.2, 133.3, 137.2, 139.1, 155.2, 156.4, 160.6, 166.8, 174.8; LRMS (ESI) m/z 719 $[\text{M}+\text{H}]^+$; HRMS (ESI) calcd for $\text{C}_{41}\text{H}_{43}\text{N}_4\text{O}_8$ $[\text{M}+\text{H}]^+$ 719.3081, found 719.3111.

4.2.3 Synthesis of *methyl 3-(((2-(4-(2-(2-(4-(2-(1,3-dioxoisindolin-2-yl)ethyl)-1H-1,2,3-triazol-1-yl)ethoxy)ethoxy)phenyl)-4-oxo-4H-chromen-3-yl)oxy)methyl)benzoate* (**Ac19Az8**):

This compound (55 mg) was obtained from **Ac19** and **Az8** in 77 % yield according to the general

procedure described above. ¹H NMR (500 MHz, CDCl₃) δ 3.10 (t, *J* = 7.08 Hz, 2 H), 3.79 - 3.85 (m, 2 H), 3.85 - 3.89 (m, 3 H), 3.91 - 3.98 (m, 4 H), 4.15 (dd, *J* = 5.12, 3.66 Hz, 2 H), 4.54 (t, *J* = 4.88 Hz, 2 H), 5.14 (s, 2 H), 6.93 - 6.98 (m, 2 H), 7.34 (t, *J* = 7.57 Hz, 1 H), 7.38 - 7.43 (m, 1 H), 7.50 (d, *J* = 8.79 Hz, 1 H), 7.57 - 7.62 (m, 2 H), 7.62 - 7.69 (m, 3 H), 7.73 - 7.77 (m, 2 H), 7.91 (dt, *J* = 7.81, 1.46 Hz, 1 H), 7.96 - 8.02 (m, 3 H), 8.27 (dd, *J* = 8.05, 1.22 Hz, 1 H); ¹³C NMR (126 MHz, CDCl₃) δ 24.7, 37.2, 50.1, 51.9, 67.1, 69.4, 69.6, 73.1, 114.2, 117.8, 122.9, 123.3, 123.9, 124.5, 125.5, 128.1, 129.0, 129.6, 129.9, 130.4, 131.8, 133.0, 133.2, 133.7, 137.0, 138.9, 154.9, 156.1, 160.3, 166.6, 167.8, 174.6; LRMS (ESI) *m/z* 715 [M+H]⁺, 737 [M+Na]⁺; HRMS (ESI) calcd for C₄₀H₃₅N₄O₉ [M+H]⁺ 715.2404, found 715.2369; calcd for C₄₀H₃₄N₄O₉Na [M+Na]⁺ 737.2223, found 737.2195.

4.2.4 Synthesis of *methyl 3-(((2-(4-(2-(2-(2-(4-(2-(1,3-dioxoisindolin-2-yl)ethyl)-1H-1,2,3-triazol-1-yl)ethoxy)ethoxy)ethoxy)phenyl)-4-oxo-4H-chromen-3-yl)oxy)methyl)benzoate*

(Ac19Az9): This compound (62.2 mg) was obtained from **Ac19** and **Az9** in 82 % yield according to the general procedure described above. ¹H NMR (500 MHz, CDCl₃) δ 3.09 (t, *J* = 7.32 Hz, 2 H), 3.61 - 3.65 (m, 2 H), 3.68 - 3.72 (m, 2 H), 3.84 - 3.89 (m, 7 H), 3.97 (t, *J* = 7.57 Hz, 2 H), 4.18 - 4.22 (m, 2 H), 4.48 - 4.53 (m, 2 H), 5.13 (s, 2 H), 6.94 - 6.99 (m, 2 H), 7.34 (t, *J* = 7.57 Hz, 1 H), 7.38 - 7.43 (m, 1 H), 7.51 (d, *J* = 8.30 Hz, 1 H), 7.57 - 7.70 (m, 5 H), 7.78 (dd, *J* = 5.37, 2.93 Hz, 2 H), 7.92 (dt, *J* = 7.81, 1.46 Hz, 1 H), 7.94 - 7.99 (m, 3 H), 8.28 (dd, *J* = 8.05, 1.71 Hz, 1 H); ¹³C NMR (126 MHz, CDCl₃) δ 24.9, 29.7, 37.4, 50.2, 52.0, 67.5, 69.6, 69.6, 70.6, 70.7, 73.3, 114.4, 117.9, 123.2, 123.4, 124.2, 124.7, 125.8, 128.3, 129.3, 129.8, 130.1, 130.5, 132.0, 133.2, 133.3, 133.9, 137.2, 139.1, 155.2, 156.4, 160.6, 166.8, 168.1, 174.8; LRMS (ESI) *m/z* 759 [M+H]⁺, 781 [M+Na]⁺; HRMS (ESI) calcd for C₄₂H₃₉N₄O₁₀ [M+H]⁺ 759.2666, found 759.2631; calcd for C₄₂H₃₈N₄O₁₀Na [M+Na]⁺ 781.2486, found 781.2448.

4.2.5 Synthesis of methyl 3-(((2-(4-(2-(2-(4-((dibenzylamino)methyl)-1H-1,2,3-triazol-1-yl)ethoxy)ethoxy)phenyl)-4-oxo-4H-chromen-3-yl)oxy)methyl)benzoate (Ac20Az8): This compound (44.3 mg) was obtained from **Ac20** and **Az8** in 59 % yield according to the general procedure described above. ¹H NMR (500 MHz, CDCl₃) δ 3.59 (s, 4 H), 3.74 (s, 2 H), 3.82 (dd, *J* = 5.37, 3.90 Hz, 2 H), 3.87 (s, 3 H), 3.97 (t, *J* = 5.12 Hz, 2 H), 4.08 - 4.13 (m, 2 H), 4.57 (t, *J* = 5.12 Hz, 2 H), 5.14 (s, 2 H), 6.88 - 6.92 (m, 2 H), 7.20 (d, *J* = 6.83 Hz, 2 H), 7.27 - 7.30 (m, 4 H), 7.32 - 7.40 (m, 5 H), 7.42 (s, 1 H), 7.51 (d, *J* = 8.30 Hz, 1 H), 7.57 - 7.63 (m, 2 H), 7.68 (s, 1 H), 7.90 - 7.99 (m, 4 H), 8.29 (dd, *J* = 8.05, 1.71 Hz, 1 H); ¹³C NMR (126 MHz, CDCl₃) δ 48.2, 50.2, 52.0, 57.7, 67.3, 69.7, 69.9, 73.3, 114.3, 117.9, 123.6, 124.2, 124.7, 125.8, 126.9, 128.2, 128.3, 128.7, 129.3, 129.8, 130.1, 130.6, 133.2, 133.4, 137.2, 139.1, 139.3, 145.5, 155.2, 156.4, 160.4, 166.8, 174.9; LRMS (ESI) *m/z* 751 [M+H]⁺; HRMS (ESI) calcd for C₄₅H₄₃N₄O₇ [M+H]⁺ 751.3132, found 751.3105.

4.2.6 Synthesis of methyl 3-(((4-oxo-2-(4-(2-(2-(4-((phenylamino)methyl)-1H-1,2,3-triazol-1-yl)ethoxy)ethoxy)phenyl)-4H-chromen-3-yl)oxy)methyl)benzoate (Ac27Az8): This compound (71 mg) was obtained from **Ac27** and **Az8** in 79 % yield according to the general procedure described above. ¹H NMR (400 MHz, CDCl₃) δ 3.76 - 3.82 (m, 2 H), 3.88 (s, 3 H), 3.91 - 3.99 (m, 2 H), 4.05 - 4.13 (m, 2 H), 4.24 (br. s., 1 H), 4.41 (s, 2 H), 4.54 (t, *J* = 4.89 Hz, 2 H), 5.15 (s, 2 H), 6.63 (d, *J* = 8.07 Hz, 2 H), 6.69 (t, *J* = 7.21 Hz, 1 H), 6.93 (d, *J* = 9.05 Hz, 2 H), 7.13 (t, *J* = 7.82 Hz, 2 H), 7.35 (t, *J* = 7.70 Hz, 1 H), 7.42 (t, *J* = 7.58 Hz, 1 H), 7.51 (d, *J* = 8.31 Hz, 1 H), 7.60 (d, *J* = 7.58 Hz, 1 H), 7.64 (s, 1 H), 7.65 - 7.72 (m, 1 H), 7.90 - 8.01 (m, 4 H), 8.29 (d, *J* = 7.83 Hz, 1 H); ¹³C NMR (101 MHz, CDCl₃) δ 39.8, 50.2, 52.0, 67.2, 69.6, 69.7, 73.3, 142.4, 113.1, 114.3, 117.9, 117.9, 122.8, 123.5, 124.1, 124.7, 125.7, 128.3, 129.2, 129.2, 129.8, 130.1, 130.5, 133.2,

133.3, 137.1, 139.1, 146.1, 147.6, 155.2, 156.3, 160.4, 166.8, 174.8; LRMS (ESI) m/z 647 [M+H]⁺; HRMS (ESI) calcd for C₃₇H₃₅N₄O₇ [M+H]⁺ 647.2506, found 647.2513.

4.2.7 Synthesis of methyl 3-(((2-(4-(4-(1-(2-(2-hydroxyethoxy)ethyl)-1H-1,2,3-triazol-4-yl)butoxy)phenyl)-4-oxo-4H-chromen-3-yl)oxy)methyl)benzoate (Ac32Az16): This compound (40 mg) was obtained from **Ac32** and **Az16** in 85 % yield according to the general procedure described above. ¹H NMR (500 MHz, CDCl₃) δ 1.88 (br. s., 4 H), 2.79 (br. s., 2 H), 3.51 - 3.59 (t, $J = 2.54$ Hz, 2 H), 3.70 (t, $J = 2.52$ Hz, 2 H), 3.83 - 3.90 (m, 5 H), 4.03 (t, $J = 3.54$ Hz, 2 H), 4.51 (br. s., 2 H), 5.11 (s, 2 H), 6.91 (d, $J = 8.79$ Hz, 2 H), 7.32 (t, $J = 2.43$ Hz, 1 H), 7.38 (t, $J = 7.57$ Hz, 1 H), 7.49 (d, $J = 8.30$ Hz, 1 H), 7.57 (d, $J = 7.81$ Hz, 1 H), 7.62 - 7.67 (m, 1 H), 7.90 (d, $J = 7.81$ Hz, 1 H), 7.95 (d, $J = 8.79$ Hz, 3 H), 8.25 (d, $J = 7.81$ Hz, 1 H); ¹³C NMR (126 MHz, CDCl₃) δ 25.2, 25.8, 28.6, 50.1, 52.0, 61.5, 67.6, 69.3, 72.4, 73.3, 114.2, 117.9, 122.9, 124.0, 124.6, 125.6, 128.2, 129.2, 129.7, 130.0, 130.4, 133.2, 133.3, 137.1, 138.9, 155.1, 156.6, 160.9, 166.8, 174.8; LRMS (ESI) m/z 614 [M+H]⁺; HRMS (ESI) calcd for C₃₄H₃₆N₃O₈ [M+H]⁺ 614.2513, found 614.2506.

4.2.8 Synthesis of Methyl 3-(((2-(4-(4-(1-benzyl-1H-1,2,3-triazol-4-yl)butoxy)phenyl)-4-oxo-4H-chromen-3-yl)oxy)methyl)benzoate (Ac32Az19): This compound (20 mg) was obtained from **Ac32** and **Az19** in 82 % yield according to the general procedure described above. ¹H NMR (400 MHz, CDCl₃) δ 1.84 - 1.89 (br. s., 4 H), 2.75 - 2.82 (t, $J = 5.21$ Hz, 2 H), 3.86 (s, 3 H), 4.04 (t, $J = 3.56$ Hz, 2 H), 5.13 (s, 2 H), 5.49 (s, 2 H), 6.89 - 6.93 (m, 2 H), 7.23 - 7.27 (m, 3 H), 7.31 - 7.36 (m, 4 H), 7.38 - 7.43 (m, 1 H), 7.51 (d, $J = 8.07$ Hz, 1 H), 7.59 (d, $J = 7.83$ Hz, 1 H), 7.67 (ddd, $J = 8.44, 6.97, 1.71$ Hz, 1 H), 7.92 (d, $J = 7.82$ Hz, 1 H), 7.94 - 8.01 (m, 3 H), 8.27 (dd, $J = 8.07, 1.22$ Hz, 1 H); ¹³C NMR (101 MHz, CDCl₃) δ 25.3, 25.8, 28.6, 52.0, 54.0, 67.6, 73.3, 114.2, 117.9,

120.6, 122.9, 124.1, 124.6, 125.7, 127.9, 128.3, 128.6, 129.0, 129.2, 129.8, 130.0, 130.5, 133.2, 133.3, 134.8, 137.1, 138.9, 155.1, 156.6, 160.9, 166.8, 174.9; LRMS (ESI) m/z 616 [M+H]⁺; HRMS (ESI) calcd for C₃₇H₃₄N₃O₆ [M+H]⁺ 616.2419, found 616.2411.

4.2.9 Synthesis of methyl 3-(((2-(4-(2-(2-(2-(4-(4-(4-formylphenoxy)butyl)-1H-1,2,3-triazol-1-yl)ethoxy)ethoxy)ethoxy)phenyl)-4-oxo-4H-chromen-3-yl)oxy)methyl)benzoate (Ac33Az9):

This compound (35 mg) was obtained from **Ac33** and **Az9** in 87 % yield according to the general procedure described above. ¹H NMR (500 MHz, CDCl₃) δ 1.84 (br. s., 4 H), 2.75 (br. s., 2 H), 3.59 - 3.66 (m, 2 H), 3.66 - 3.72 (m, 2 H), 3.81 - 3.90 (m, 7 H), 4.01 (t, $J = 4.80$ Hz, 2 H), 4.17 (t, $J = 4.39$ Hz, 2 H), 4.50 (t, $J = 4.88$ Hz, 2 H), 5.13 (s, 2 H), 6.95 (d, $J = 8.79$ Hz, 2 H), 6.92 (d, $J = 8.30$ Hz, 2 H), 7.33 (t, $J = 7.57$ Hz, 1 H), 7.40 (t, $J = 7.32$ Hz, 1 H), 7.49 (d, $J = 8.30$ Hz, 2 H), 7.58 (d, $J = 7.32$ Hz, 1 H), 7.66 (t, $J = 7.81$ Hz, 1 H), 7.77 (d, $J = 8.30$ Hz, 2 H), 7.91 (d, $J = 7.32$ Hz, 1 H), 7.93 - 8.02 (m, 3 H), 8.26 (d, $J = 7.81$ Hz, 1 H), 9.82 (s, 1 H); ¹³C NMR (126 MHz, CDCl₃) δ 25.2, 25.8, 28.5, 52.0, 67.5, 67.9, 69.5, 69.6, 70.5, 70.7, 73.3, 114.3, 114.6, 117.9, 123.4, 124.1, 124.7, 125.7, 128.3, 129.2, 129.7, 129.8, 130.1, 130.5, 131.9, 133.2, 133.3, 137.1, 139.0, 155.1, 156.3, 160.6, 164.0, 166.8, 174.8, 190.7; LRMS (ESI) m/z 762 [M+H]⁺; HRMS (ESI) calcd for C₄₃H₄₄N₃O₁₀ [M+H]⁺ 762.8214, found 762.8205.

4.2.10 Synthesis of methyl 3-(((2-(4-(2-(2-(2-(4-((benzyl(2-hydroxyethyl)amino)methyl)-1H-1,2,3-triazol-1-yl)ethoxy)ethoxy)ethoxy)phenyl)-4-oxo-4H-chromen-3-yl)oxy)methyl)benzoate (Ac36Az9):

This compound (60 mg) was obtained from **Ac36** and **Az9** in 72 % yield according to the general procedure described above. ¹H NMR (600 MHz, CDCl₃) δ 2.75 (t, $J = 5.14$ Hz, 2 H), 3.62 - 3.67 (m, 4 H), 3.69 - 3.73 (m, 4 H), 3.84 - 3.87 (m, 4 H), 3.87 - 3.92 (m, 6 H), 4.16 - 4.20 (m, 2 H), 4.53 - 4.57 (m, 2 H), 5.15 (s, 2 H), 6.97 (s, 1 H), 6.95 (s, 1 H), 7.24 - 7.28 (m, 1 H), 7.30

- 7.37 (m, 5 H), 7.42 (t, $J = 7.34$ Hz, 1 H), 7.53 (d, $J = 8.80$ Hz, 1 H), 7.60 (d, $J = 7.34$ Hz, 1 H), 7.66 - 7.71 (m, 2 H), 7.94 (d, $J = 7.34$ Hz, 1 H), 7.99 (d, $J = 8.80$ Hz, 3 H), 8.29 (d, $J = 8.80$ Hz, 1 H); ^{13}C NMR (151 MHz, CDCl_3) δ 47.9, 50.2, 52.0, 54.7, 57.8, 58.4, 67.3, 69.4, 69.5, 70.5, 70.6, 73.2, 114.2, 117.9, 123.3, 124.0, 124.0, 124.6, 125.6, 127.4, 128.2, 128.4, 129.1, 129.2, 129.7, 130.0, 130.5, 133.2, 133.3, 137.0, 138.9, 155.1, 156.4, 160.5, 166.8, 174.8. LRMS (ESI) m/z 749 $[\text{M}+\text{H}]^+$; HRMS (ESI) calcd for $\text{C}_{42}\text{H}_{45}\text{N}_4\text{O}_9$ $[\text{M}+\text{H}]^+$ 749.3211, found 749.3208.

4.3. Materials for Biological Studies

Dimethyl sulfoxide (DMSO), paclitaxel, topotecan, doxorubicin (DOX), mitoxantrone, quercetin, PSC833, verapamil, Ko143 and phenazine methosulfate (PMS) were purchased from Sigma-Aldrich. Disuccinimidyl suberate (DSS) was purchased from Thermofisher. Hoechst 33342 was purchased from Molecular Probes. Dulbecco's Modified Eagle's Medium (DMEM), trypsin-ethylenediaminetetraacetic acid (EDTA) and penicillin/streptomycin were purchased from Gibco BRL. Roswell Park Memorial Institute (RPMI) 1640 medium and fetal bovine serum (FBS) was purchased from HyClone Laboratories. 3-(4,5-Dimethylthiazol-2-yl)-5-[3-(carboxymethoxy)phenyl]-2-(4-sulfo-phenyl)-2H-tetrazolium (MTS) was purchased from Promega. Phosphate-buffered saline (PBS) was made by dissolving 8 g of sodium chloride, 0.2 g of potassium chloride, 1.44 g of disodium hydrogen phosphate and 0.24 g of potassium dihydrogen phosphate in 1000 mL of distilled water and sterilized by autoclaving. The human breast cancer cell lines LCC6 and P-gp transfectant LCC6MDR were kindly provided by Prof. R. Clarke (Georgetown University Medical School, USA). The human ovarian carcinoma cell line 2008/MRP1 was generous gift from Prof. P. Borst (The Netherlands Cancer Institute, Amsterdam, Netherlands). The human embryonic kidney cell lines HEK293/pcDNA3.1, BCRP-transfectant

HEK293/R2, MCF7-MX100 and S1M180 cells were generously provided by Dr. Kenneth To (The Chinese University of Hong Kong, Hong Kong). L929 cell line was purchased from ATCC.

4.4. Cell Culture

HEK293/R2, HEK293/pcDNA3.1, MCF7-MX100, 2008/MRP1 and S1M180 cells were cultured in RPMI 1640 medium with 10 % FBS and 100 U/mL penicillin and 100 µg/mL of streptomycin and maintained at 37 °C in a humidified atmosphere with 5 % CO₂. The L929 and LCC6MDR cells were cultured in DMEM supplemented with 10 % FBS and 100 U/mL penicillin and 100 µg/mL of streptomycin and maintained at 37 °C in a humidified atmosphere with 5 % CO₂. For each passage of HEK293pcDNA3.1 or HEK293/R2, 1 mg/mL G418 was added to culture. The cells were split constantly after a confluent monolayer had been formed. To split cells, the plate was washed briefly with phosphate-buffered saline (PBS), treated with 0.05 % trypsin-EDTA and harvested by centrifugation.

4.5. EC₅₀ determination

5,000 cells of HEK293/R2 in each well of 96-well plate were incubated with different concentrations of topotecan (0, 8, 25, 74, 222, 667 and 2000 nM) and modulators (0, 1.6, 8, 40, 200, 1000 nM). 7,500 cells of MCF7-MX100 were incubated with different concentrations of topotecan (0, 0.41, 1.2, 3.7, 11, 33 and 100 µM) and modulators (0, 1.6, 8, 40, 200, 1000 nM). 4,000 cells of 2008/MRP1 were incubated with various doses of DOX (0, 8, 25, 74, 222, 667 and 2000 nM) and modulators (0, 62.5, 125, 250, 500, 1000 nM). 6,500 cells of LCC6MDR were incubated with various doses of paclitaxel (0, 1.6, 5, 15, 15, 44, 133 and 400 nM) and modulators (0, 62.5, 125, 250, 500, 1000 nM). The final volume in each well of 96-well plates was 200 µL. The plates were then incubated for 5 days at 37 °C.

The CellTiter 96 A_{queous} Assay (Promega) was used to measure the cell proliferation according to the manufacturer's instructions. MTS (2 mg/mL) and PMS (0.92 mg/mL) were mixed in a ratio of 20:1. An aliquot (10 μ L) of the freshly prepared MTS/PMS mixture was added into each well, and the plate was incubated for 2 hr at 37 °C. Optical absorbance at 490 nm was recorded with microplate absorbance reader (Bio-Rad). All experiments were performed in triplicate and repeated at least twice and the results were represented as mean \pm standard error of mean. The EC₅₀ value was determined by PRISM software.

4.6. Mitoxantrone sensitization assay

5,000 cells of HEK293/R2, 4,000 cells of 2008MRP1 or 6,500 cells of LCC6MDR cells were incubated with different doses of mitoxantrone with or without 1 μ M triazole-bridged flavonoids or Ko143 for 5 days. The final volume in each well of 96-well plates was 200 μ L. For determining EC₅₀ value, the cells were incubated with different doses of mitoxantrone and modulators together. The % of survival and EC₅₀ values was determined as mentioned previously.

4.7. Topotecan and mitoxantrone accumulation assay

Topotecan or mitoxantrone accumulation assay was done in 1 mL volume. A 5×10^5 cells of HEK293/pcDNA3.1 or HEK293/R2 cells were added in an Eppendorf tube and incubated with 50 μ M topotecan or 5 μ M mitoxantrone and 1 or 2 μ M of triazole-bridged flavonoids or Ko143 at 37 °C for 2 hr. A 0.2 % DMSO was used as a negative control. After incubation, the cells were spun down and washed with cold PBS, pH 7.4 for one time and then resuspended with 200 μ L of cold FACS buffer (1 % BSA and 1 mM EDTA in PBS). The intracellular topotecan or mitoxantrone levels were analyzed by BD C6 Accuri flow cytometer using FL1 channel and FL4 respectively. For each sample, a total of 50,000 events was collected.

4.8. Determination of surface BCRP protein expression

40,000 cells of HEK293/pcDNA3.1 and HEK293/R2 cells were seeded in a 6-well plate and incubated with 0, 1 or 3 μM of triazole-bridged flavonoids for 24 hr, respectively. After 24 hr, the cells were trypsinized and washed once with 1X PBS. After spinning, the cells were resuspended in 50 μL FACS buffer (1 % BSA and 1 mM EDTA in PBS) and stained with 1 μL FITC mouse anti-human BCRP antibody (Miltenyi Biotec) at 4 $^{\circ}\text{C}$ for 45 min. After staining, the cells were washed once with 500 μL cold FACS buffer and resuspended in 200 μL FACS buffer. IgG2b-FITC was used as an isotype control. The BCRP-FITC level was analyzed by BD C6 Accuri flow cytometer using FL1 channel at EX 480 nm and EM 533/30 nm. For each sample, a total of 50,000 events was collected.

4.9. Mitoxantrone efflux study

To measure the mitoxantrone efflux, HEK293/pcDNA3.1 or HEK293/R2 cells were pre-loaded with 5 μM of mitoxantrone for 1 hr at 37 $^{\circ}\text{C}$. Then, the cells were spun down and washed once with cold PBS. Then the cells were further incubated in drug-free media with or without compound **Ac32Az19** (2 μM). At 0, 30, 60, 90, 120 and 150 min, 1×10^6 cells in 1 mL volume were harvested for measuring the intracellular mitoxantrone concentration. The % of mitoxantrone reduction was calculated = [(mitoxantrone level at final time point / mitoxantrone level at 0 min) * 100%]. The mitoxantrone level was determined by C6 Accuri flow cytometer at FL4 channel as described previously.

4.10. Vanadate-sensitive BCRP-ATPase activity

5×10^7 cells of S1M180 were resuspended in 5 mL homogenization buffer (0.33 M sucrose, 300 mM Tris pH7.4, 1 mM EDTA, 1 mM EGTA, 2 mM DTT, 100 mM 6-aminocaproic acid, 1mM PMSF and 1x protease inhibitor (cOmplete™ Protease Inhibitor Cocktail Tablets, Roche) and lysed using a Branson SFX550 sonicator for 10 cycles at 50 % amplitude with 30 seconds on / 30 seconds off. Lysate was centrifuged at 3,500 x g for 10 min at 4°C. Membrane fraction of cells was collected by ultracentrifugation of cell lysate at 45,000 rpm using Himac CP70G (Hitachi) for 1.5 hr. Membrane fraction pellet was re-suspended in 300 µL of ATPase assay buffer (50 mM Tris at pH7.5, 2 mM EGTA at pH 7.0, 2 mM DTT, 50 mM KCl, 10 mM MgCl₂, 5 mM sodium azide, and 1 mM ouabain). Protein concentration was determined by Bradford assay. Membrane fraction was pre-incubated with or without 0.3 mM sodium *orthovanadate* and respective tested compounds for 30 min. Then, 2.5 mM ATP was added to each well and the plate was further incubated for 1 hr at 37°C. Reactions were stopped by adding 200 µL freshly prepared cold stop buffer (0.2 % ammonium molybdate, 1.4 % sulphuric acid, 0.9 % SDS and 1 % ascorbic acid) and incubated at room temperature for 15 min. Absorbance of 655 nm was measured by CLARIOstar® microplate reader (BMG).

4.11. Determination of intracellular Ac32Az19 level using ultra-performance liquid chromatography-mass spectrometry (UPLC-MS/MS)

1×10^7 cells of HEK293/pcDNA3.1 and HEK293/R2 were incubated with 2 µM or 10 µM of **Ac32Az19** at 37 °C for 2 hr. The final volume is 1 mL in RPMI1640 media. After 2 hr, the cells were spun down and the supernatant was removed. To cell pellet, 1 mL cold PBS was added to wash out the **Ac32Az19**. The cells were then lysed with 400 µL of 100 % acetonitrile and vortexed

for 1 min at room temperature. After lysing, the cells were spun down at 14,000 rpm for 10 min at room temperature. The supernatant was saved and passed through 0.22 μm filter. The intracellular **Ac32Az19** level was then analyzed by UPLC-MS/MS. UPLC (Acquity Waters) and triple quadrupole mass analyzer (Quattro Ultra) with an electrospray ionization source in positive mode were used to quantify **Ac32Az19**. Acquity UPLC BEH C8 (1.7 μm 2.1 x 50 mm) from Waters was used to separate **Ac32Az19**. Mobile phase used for **Ac32Az19** analysis included water and acetonitrile. **Ac32Az19** was monitored at m/z 616 \rightarrow m/z 149.

4.12. 5D3 shift assay

5×10^5 cells of HEK293/R2 were resuspended with 98 μL FACS buffer (0.1 % BSA and 1 mM EDTA in 1X PBS) and pre-incubated at 37 $^\circ\text{C}$ (with shaking at 200 rpm) with respective concentration of Ko143 (1 μM), GF120918 (1 μM), **Ac32Az19** (1 μM), quercetin (10 μM), Hoechst 33342 (10 μM), PSC833 (1 μM) and verapamil (1 μM) for 15 min. After 15 min, 1 μL diluted FITC mouse anti-human BCRP antibody (Clone 5D3/CD338, Miltenyi Biotec, 130-105-009) (1:2 dilution) was added and further incubated for 30 min at 37 $^\circ\text{C}$ (with shaking at 200 rpm). At the same time, cells containing only with inhibitors or substrates were included for measuring FITC background level of compounds. After staining, the cells were washed once with 500 μL cold FACS buffer and resuspended in 200 μL FACS buffer. The BCRP-FITC level was analyzed by BD C6 Accuri flow cytometer using FL1 channel at EX 480 nm and EM 533/30 nm. For each sample, a total of 50,000 events was collected. Net 5D3 labeling of compound was calculated = (FITC level in the presence of compounds and BCRP-FITC antibody) – (FITC level in the presence of compounds only). 5D3 shift level of compound was calculated = (Net 5D3 labeling of compound – Net 5D3 labeling of untreated DMSO control). The % of 5D3 shift

relative to 1 μ M Ko143 was calculated = [(5D3 shift level of compound / 5D3 shift level of Ko143) * 100%].

4.13 Chemical cross-linking of BCRP oligomer

2 x 10⁵ HEK293/R2 cells were seeded into each well of 6-well plate and incubated overnight at 37 °C with 5% CO₂. Then, the cells were treated with 1 μ M of **Ac32Az19**, Ko143 or 0.1 % DMSO for 4 days. After 4 days treatment, the cells were further incubated with or without chemical cross-linking reagent DSS for 45 min at room temperature with shaking.⁶⁴ After 45 min, the cross-linking reaction was stopped by incubating the cells with 50 mM glycine and 20 mM Tris-HCl pH 7.6 for 15 min. Then, the cells were washed twice with KCl/Hepes buffer (90 mM KCl, 50 mM Hepes, pH 7.5). After washing, the cells were lysed with 200 μ L RIPA buffer for 10 min on ice. The protein amount in the whole cell lysate was determined using Bradford assay. About 50 μ g of whole cell lysate was run on the 10 % SDS-PAGE. The protein level of BCRP monomer and oligomer were analyzed by Western blot using anti-BCRP antibody (Santa Cruz, sc-58222, 1:200 dilution). The β -actin level was also determined using anti- β -actin antibody (Santa Cruz, sc-47778, 1:200 dilution). Finally, the protein amount of BCRP and β -actin in each sample lane of Western blot was analyzed by ImageJ software. After 4-day treatment with modulators, the cells were washed 2 times with 8 mL 1X PBS and then harvested to do the mitoxantrone accumulation assay and its intracellular level was measured by flow cytometry as described as above.

ASSOCIATED CONTENT

Supporting Information

The Supporting Information is available free of charge via the Internet at <http://pubs.acs.org>.

^1H NMR and ^{13}C NMR spectra of all representative compounds listed in Table 2.

SMILES molecular strings formulas (CSV).

AUTHOR INFORMATION

Corresponding authors

*For L. M. C. C, Phone: (852)-34008662; Fax: (852)-23649932;

E-mail: larry.chow@polyu.edu.hk

*For T. H. C, Phone: (852)-34008670; Fax: (852)-23649932;

E-mail: tak-hang.chan@polyu.edu.hk

ORCID

Larry M. C. Chow: 000-0002-9222-8322

Tak Hang Chan: 0000-0002-8702-4499

Author contribution

¹Iris L. K. Wong, ¹Xuezhen Zhu, and ¹Kin-Fai Chan contributed equally to this work. The manuscript was written through contributions of all authors. All authors have given approval to the final version of the manuscript.

Notes

The authors declare no competing financial interest. The patent US 9611256 B1 associated with this manuscript has been licensed to Athenex Inc.

ACKNOWLEDGEMENTS

The work described in this paper was supported by the Hong Kong Research Grant Council General Research Fund (B-Q21B), Early Career Scheme (25100014) and Hong Kong Polytechnic University internal grant (GU383). We thank University Research Facilities of Life Science (ULS) of The Hong Kong Polytechnic University for providing the flow cytometry service and mass spectrometry service.

ABBREVIATIONS USED

BCRP, Breast cancer resistance protein; MRP1, multidrug resistance protein-1; P-gp, P-glycoprotein; MDR, multidrug resistance; ABC, ATP-binding cassette; EC₅₀, effective concentration; RPMI1640, Roswell Park Memorial Institute 1640; doxorubicin, DOX, MTS, [3-(4,5-dimethylthiazol-2-yl)-5-(3-carboxymethoxyphenyl)-2-(4-sulfophenyl)-2H-tetrazolium, inner salt.

References

1. Borst, P.; Elferink, R. O. Mammalian ABC transporters in health and disease. *Annu Rev Biochem* **2002**, *71*, 537-592.
2. Borst, P.; Evers, R.; Kool, M.; Wijnholds, J. A family of drug transporters: the multidrug resistance-associated proteins. *J Natl Cancer Inst* **2000**, *92*, 1295-1302.
3. Domenichini, A.; Adamska, A.; Falasca, M. ABC transporters as cancer drivers: potential functions in cancer development. *Biochim Biophys Acta Gen Subj* **2019**, *1863*, 52-60.
4. Mao, Q.; Unadkat, J. D. Role of the breast cancer resistance protein (BCRP/ABCG2) in drug transport--an update. *Aaps j* **2015**, *17*, 65-82.
5. McDevitt, C. A.; Collins, R.; Kerr, I. D.; Callaghan, R. Purification and structural analyses of ABCG2. *Adv Drug Deliv Rev* **2009**, *61*, 57-65.
6. Dezi, M.; Fribourg, P. F.; Di Cicco, A.; Arnaud, O.; Marco, S.; Falson, P.; Di Pietro, A.; Levy, D. The multidrug resistance half-transporter ABCG2 is purified as a tetramer upon selective extraction from membranes. *Biochim Biophys Acta* **2010**, *1798*, 2094-2101.
7. Rosenberg, M. F.; Bikadi, Z.; Chan, J.; Liu, X.; Ni, Z.; Cai, X.; Ford, R. C.; Mao, Q. The human breast cancer resistance protein (BCRP/ABCG2) shows conformational changes with mitoxantrone. *Structure* **2010**, *18*, 482-493.
8. Wong, K.; Briddon, S. J.; Holliday, N. D.; Kerr, I. D. Plasma membrane dynamics and tetrameric organisation of ABCG2 transporters in mammalian cells revealed by single particle imaging techniques. *Biochim Biophys Acta* **2016**, *1863*, 19-29.
9. Galimberti, S.; Nagy, B.; Benedetti, E.; Pacini, S.; Brizzi, S.; Caracciolo, F.; Papineschi, F.; Ciabatti, E.; Guerrini, F.; Fazzi, R.; Canestraro, M.; Petrini, M. Evaluation of the MDR1, ABCG2, topoisomerases II alpha and GSTpi gene expression in patients affected by aggressive mantle cell lymphoma treated by the R-Hyper-CVAD regimen. *Leuk Lymphoma* **2007**, *48*, 1502-1509.

10. Kim, Y. H.; Ishii, G.; Goto, K.; Ota, S.; Kubota, K.; Murata, Y.; Mishima, M.; Saijo, N.; Nishiwaki, Y.; Ochiai, A. Expression of breast cancer resistance protein is associated with a poor clinical outcome in patients with small-cell lung cancer. *Lung Cancer* **2009**, *65*, 105-111.
11. Kovalev, A. A.; Tsvetaeva, D. A.; Grudinskaja, T. V. Role of ABC-cassette transporters (MDR1, MRP1, BCRP) in the development of primary and acquired multiple drug resistance in patients with early and metastatic breast cancer. *Exp Oncol* **2013**, *35*, 287-290.
12. Lee, S. H.; Kim, H.; Hwang, J. H.; Lee, H. S.; Cho, J. Y.; Yoon, Y. S.; Han, H. S. Breast cancer resistance protein expression is associated with early recurrence and decreased survival in resectable pancreatic cancer patients. *Pathol Int* **2012**, *62*, 167-175.
13. Rijavec, M.; Silar, M.; Triller, N.; Kern, I.; Cegovnik, U.; Košnik, M.; Korošec, P. Expressions of topoisomerase II α and BCRP in metastatic cells are associated with overall survival in small cell lung cancer patients. *Pathol Oncol Res* **2011**, *17*, 691-696.
14. Tian, C.; Ambrosone, C. B.; Darcy, K. M.; Krivak, T. C.; Armstrong, D. K.; Bookman, M. A.; Davis, W.; Zhao, H.; Moysich, K.; Gallion, H.; DeLoia, J. A. Common variants in ABCB1, ABCC2 and ABCG2 genes and clinical outcomes among women with advanced stage ovarian cancer treated with platinum and taxane-based chemotherapy: a gynecologic oncology group study. *Gynecol Oncol* **2012**, *124*, 575-581.
15. Uggla, B.; Stahl, E.; Wagsater, D.; Paul, C.; Karlsson, M. G.; Sirsjo, A.; Tidefelt, U. BCRP mRNA expression v. clinical outcome in 40 adult AML patients. *Leuk Res* **2005**, *29*, 141-146.
16. Yoh, K.; Ishii, G.; Yokose, T.; Minegishi, Y.; Tsuta, K.; Goto, K.; Nishiwaki, Y.; Kodama, T.; Suga, M.; Ochiai, A. Breast cancer resistance protein impacts clinical outcome in platinum-based chemotherapy for advanced non-small cell lung cancer. *Clin Cancer Res* **2004**, *10*, 1691-1697.
17. Allikmets, R.; Schriml, L. M.; Hutchinson, A.; Romano-Spica, V.; Dean, M. A human placenta-specific ATP-binding cassette gene (ABCP) on chromosome 4q22 that is involved in multidrug resistance. *Cancer Res* **1998**, *58*, 5337-5339.

18. Doyle, L. A.; Yang, W.; Abruzzo, L. V.; Krogmann, T.; Gao, Y.; Rishi, A. K.; Ross, D. D. A multidrug resistance transporter from human MCF-7 breast cancer cells. *Proc Natl Acad Sci U S A* **1998**, *95*, 15665-15670.
19. Miyake, K.; Mickley, L.; Litman, T.; Zhan, Z.; Robey, R.; Cristensen, B.; Brangi, M.; Greenberger, L.; Dean, M.; Fojo, T.; Bates, S. E. Molecular cloning of cDNAs which are highly overexpressed in mitoxantrone-resistant cells: demonstration of homology to ABC transport genes. *Cancer Res* **1999**, *59*, 8-13.
20. Ni, Z.; Bikadi, Z.; Rosenberg, M. F.; Mao, Q. Structure and function of the human breast cancer resistance protein (BCRP/ABCG2). *Curr Drug Metab* **2010**, *11*, 603-617.
21. Robey, R. W.; Honjo, Y.; Morisaki, K.; Nadjem, T. A.; Runge, S.; Risbood, M.; Poruchynsky, M. S.; Bates, S. E. Mutations at amino-acid 482 in the ABCG2 gene affect substrate and antagonist specificity. *Br J Cancer* **2003**, *89*, 1971-1978.
22. Litman, T.; Brangi, M.; Hudson, E.; Fetsch, P.; Abati, A.; Ross, D. D.; Miyake, K.; Resau, J. H.; Bates, S. E. The multidrug-resistant phenotype associated with overexpression of the new ABC half-transporter, MXR (ABCG2). *J Cell Sci* **2000**, *113*, 2011-2021.
23. Rabindran, S. K.; He, H.; Singh, M.; Brown, E.; Collins, K. I.; Annable, T.; Greenberger, L. M. Reversal of a novel multidrug resistance mechanism in human colon carcinoma cells by fumitremorgin C. *Cancer Res* **1998**, *58*, 5850-5858.
24. Robey, R. W.; To, K. K.; Polgar, O.; Dohse, M.; Fetsch, P.; Dean, M.; Bates, S. E. ABCG2: a perspective. *Advanced drug delivery reviews* **2009**, *61*, 3-13.
25. Ito, F.; Miura, M.; Fujioka, Y.; Abumiya, M.; Kobayashi, T.; Takahashi, S.; Yoshioka, T.; Kameoka, Y.; Takahashi, N. The BCRP inhibitor febuxostat enhances the effect of nilotinib by regulation of intracellular concentration. *Int J Hematol* **2021**, *113*, 100-105.

26. National Cancer Institute. *A Phase I Study of Continuous Intravenous Infusion of PSC 833 and Vinblastine in Patients With Metastatic Renal Cancer (Feb 1997 – Jan 2001)*, Identifier: NCT00001570. <https://clinicaltrials.gov/ct2/show/NCT00001570?term=PSC833&draw=2&rank=7>.
27. National Cancer Institute. *Phase I Trial of Tariquidar (XR9576) in Combination With Doxorubicin, Vinorelbine, or Docetaxel in Pediatric Patients With Solid Tumors (Feb 2001- Jan 2016)*, Identifier: NCT00011414. <https://clinicaltrials.gov/ct2/show/NCT00011414?term=Pgp+inhibitor&cond=cancer&draw=2&rank=2>.
28. National Cancer Institute. *A Phase I Study of Infusional Chemotherapy With the P-Glycoprotein Antagonist PSC 833 (Sept 1992 – June 2002)*, Identifier: NCT00001302. <https://clinicaltrials.gov/ct2/show/NCT00001302?term=PSC833&draw=2&rank=2>.
29. Athenex, Inc. . *A Safety Study of Oraxol (HM30181 + Oral Paclitaxel) in Cancer Patients (Sept 2015 – June 2021)*, Identifier: NCT04180384. <https://clinicaltrials.gov/ct2/show/NCT04180384?term=HM30181&draw=2&rank=1>.
30. Cripe, L. D.; Uno, H.; Paietta, E. M.; Litzow, M. R.; Ketterling, R. P.; Bennett, J. M.; Rowe, J. M.; Lazarus, H. M.; Luger, S.; Tallman, M. S. Zosuquidar, a novel modulator of P-glycoprotein, does not improve the outcome of older patients with newly diagnosed acute myeloid leukemia: a randomized, placebo-controlled trial of the eastern cooperative oncology group 3999. *Blood* **2010**, 116, 4077-4085.
31. Fox, E.; Bates, S. E. Tariquidar (XR9576): a P-glycoprotein drug efflux pump inhibitor. *Expert Rev Anticancer Ther* **2007**, 7, 447-459.
32. Lhommé, C.; Joly, F.; Walker, J. L.; Lissoni, A. A.; Nicoletto, M. O.; Manikhas, G. M.; Baekelandt, M. M.; Gordon, A. N.; Fracasso, P. M.; Mietlowski, W. L.; Jones, G. J.; Dugan, M. H. Phase III study of valspodar (PSC 833) combined with paclitaxel and carboplatin compared with paclitaxel and carboplatin alone in patients with stage IV or suboptimally debulked stage III epithelial ovarian cancer or primary peritoneal cancer. *J Clin Oncol* **2008**, 26, 2674-2682.

33. Li, J.; Li, Z. N.; Du, Y. J.; Li, X. Q.; Bao, Q. L.; Chen, P. Expression of MRP1, BCRP, LRP, and ERCC1 in advanced non-small-cell lung cancer: correlation with response to chemotherapy and survival. *Clin Lung Cancer* **2009**, 10, 414-421.
34. Gottesman, M. M.; Fojo, T.; Bates, S. E. Multidrug resistance in cancer: role of ATP-dependent transporters. *Nat Rev Cancer* **2002**, 2, 48-58.
35. Rabindran, S. K.; Ross, D. D.; Doyle, L. A.; Yang, W.; Greenberger, L. M. Fumitremorgin C reverses multidrug resistance in cells transfected with the breast cancer resistance protein. *Cancer Res* **2000**, 60, 47-50.
36. Allen, J. D.; van Loevezijn, A.; Lakhai, J. M.; van der Valk, M.; van Tellingen, O.; Reid, G.; Schellens, J. H.; Koomen, G. J.; Schinkel, A. H. Potent and specific inhibition of the breast cancer resistance protein multidrug transporter in vitro and in mouse intestine by a novel analogue of fumitremorgin C. *Mol Cancer Ther* **2002**, 1, 417-425.
37. Kohler, S. C.; Wiese, M. HM30181 derivatives as novel potent and selective inhibitors of the breast cancer resistance protein (BCRP/ABCG2). *J Med Chem* **2015**, 58, 3910-3921.
38. Kannan, P.; Telu, S.; Shukla, S.; Ambudkar, S. V.; Pike, V. W.; Halldin, C.; Gottesman, M. M.; Innis, R. B.; Hall, M. D. The "specific" P-glycoprotein inhibitor tariquidar is also a substrate and an inhibitor for breast cancer resistance protein (BCRP/ABCG2). *ACS Chem Neurosci* **2011**, 2, 82-89.
39. Krapf, M. K.; Gallus, J.; Namasivayam, V.; Wiese, M. 2,4,6-substituted quinazolines with extraordinary inhibitory potency toward ABCG2. *J Med Chem* **2018**, 61, 7952-7976.
40. Krapf, M. K.; Gallus, J.; Vahdati, S.; Wiese, M. New inhibitors of breast cancer resistance protein (ABCG2) containing a 2,4-disubstituted pyridopyrimidine scaffold. *J Med Chem* **2018**, 61, 3389-3408.
41. Krapf, M. K.; Gallus, J.; Wiese, M. 4-Anilino-2-pyridylquinazolines and -pyrimidines as highly potent and nontoxic inhibitors of breast cancer resistance protein (ABCG2). *J Med Chem* **2017**, 60, 4474-4495.

42. Guragossian, N.; Belhani, B.; Moreno, A.; Nunes, M. T.; Gonzalez-Lobato, L.; Marminon, C.; Berthier, L.; Rocio Andrade Pires, A. D.; Özvegy-Laczka, C.; Sarkadi, B.; Terreux, R.; Bouaziz, Z.; Berredjem, M.; Jose, J.; Di Pietro, A.; Falson, P.; Le Borgne, M. Uncompetitive nanomolar dimeric indenoindole inhibitors of the human breast cancer resistance pump ABCG2. *Eur J Med Chem* **2020**, 113017.
43. Jabor Gozzi, G.; Bouaziz, Z.; Winter, E.; Daflon-Yunes, N.; Aichele, D.; Nacereddine, A.; Marminon, C.; Valdameri, G.; Zeinyeh, W.; Bollacke, A.; Guillon, J.; Lacoudre, A.; Pinaud, N.; Cadena, S. M.; Jose, J.; Le Borgne, M.; Di Pietro, A. Converting potent indeno[1,2-b]indole inhibitors of protein kinase CK2 into selective inhibitors of the breast cancer resistance protein ABCG2. *J Med Chem* **2015**, 58, 265-277.
44. Farzaei, M. H.; Singh, A. K.; Kumar, R.; Croley, C. R.; Pandey, A. K.; Coy-Barrera, E.; Kumar Patra, J.; Das, G.; Kerry, R. G.; Annunziata, G.; Tenore, G. C.; Khan, H.; Micucci, M.; Budriesi, R.; Momtaz, S.; Nabavi, S. M.; Bishayee, A. Targeting inflammation by flavonoids: novel therapeutic Strategy for Metabolic Disorders. *Int J Mol Sci* **2019**, 20.
45. Karthikeyan, S.; Hoti, S. L. Development of fourth generation ABC Inhibitors from natural products: a novel approach to overcome cancer multidrug resistance. *Anticancer Agents Med Chem* **2015**, 15, 605-615.
46. Kikuchi, H.; Yuan, B.; Hu, X.; Okazaki, M. Chemopreventive and anticancer activity of flavonoids and its possibility for clinical use by combining with conventional chemotherapeutic agents. *Am J Cancer Res* **2019**, 9, 1517-1535.
47. Menezes, J. C.; Orlikova, B.; Morceau, F.; Diederich, M. Natural and synthetic flavonoids: structure-activity relationship and chemotherapeutic potential for the treatment of leukemia. *Crit Rev Food Sci Nutr* **2016**, 56 Suppl 1, S4-S28.
48. Morris, M. E.; Zhang, S. Flavonoid-drug interactions: effects of flavonoids on ABC transporters. *Life Sci* **2006**, 78, 2116-2130.

49. Alvarez, A. I.; Real, R.; Perez, M.; Mendoza, G.; Prieto, J. G.; Merino, G. Modulation of the activity of ABC transporters (P-glycoprotein, MRP2, BCRP) by flavonoids and drug response. *J Pharm Sci* **2010**, *99*, 598-617.
50. Zhang, S.; Yang, X.; Coburn, R. A.; Morris, M. E. Structure activity relationships and quantitative structure activity relationships for the flavonoid-mediated inhibition of breast cancer resistance protein. *Biochem Pharmacol* **2005**, *70*, 627-639.
51. Chan, K. F.; Wong, I. L.; Kan, J. W.; Yan, C. S.; Chow, L. M.; Chan, T. H. Amine linked flavonoid dimers as modulators for P-glycoprotein-based multidrug resistance: structure-activity relationship and mechanism of modulation. *J Med Chem* **2012**, *55*, 1999-2014.
52. Chan, K. F.; Zhao, Y.; Burkett, B. A.; Wong, I. L.; Chow, L. M.; Chan, T. H. Flavonoid dimers as bivalent modulators for P-glycoprotein-based multidrug resistance: synthetic apigenin homodimers linked with defined-length poly(ethylene glycol) spacers increase drug retention and enhance chemosensitivity in resistant cancer cells. *J Med Chem* **2006**, *49*, 6742-6759.
53. Chan, K. F.; Zhao, Y.; Chow, T. W.; Yan, C. S.; Ma, D. L.; Burkett, B. A.; Wong, I. L.; Chow, L. M.; Chan, T. H. Flavonoid dimers as bivalent modulators for P-glycoprotein-based multidrug resistance: structure-activity relationships. *ChemMedChem* **2009**, *4*, 594-614.
54. Chow, L. M.; Chan, T. H. Novel classes of dimer antitumour drug candidates. *Curr Pharm Des* **2009**, *15*, 659-674.
55. Wong, I. L.; Chan, K. F.; Tsang, K. H.; Lam, C. Y.; Zhao, Y.; Chan, T. H.; Chow, L. M. Modulation of multidrug resistance protein 1 (MRP1/ABCC1)-mediated multidrug resistance by bivalent apigenin homodimers and their derivatives. *J Med Chem* **2009**, *52*, 5311-5322.
56. Wong, I. L. K.; Zhu, X.; Chan, K. F.; Law, M. C.; Lo, A. M. Y.; Hu, X.; Chow, L. M. C.; Chan, T. H. Discovery of novel flavonoid dimers to reverse multidrug resistance protein 1 (MRP1, ABCC1) mediated drug resistance in cancers using a high throughput platform with "click chemistry". *J Med Chem* **2018**, *61*, 9931-9951.

57. Zhu, X.; Wong, I. L. K.; Chan, K. F.; Cui, J.; Law, M. C.; Chong, T. C.; Hu, X.; Chow, L. M. C.; Chan, T. H. Triazole bridged flavonoid dimers as potent, nontoxic, and highly selective breast cancer resistance protein (BCRP/ABCG2) inhibitors. *J Med Chem* **2019**, *62*, 8578-8608.
58. Jackson, S. M.; Manolaridis, I.; Kowal, J.; Zechner, M.; Taylor, N. M. I.; Bause, M.; Bauer, S.; Bartholomaeus, R.; Bernhardt, G.; Koenig, B.; Buschauer, A.; Stahlberg, H.; Altmann, K. H.; Locher, K. P. Structural basis of small-molecule inhibition of human multidrug transporter ABCG2. *Nat Struct Mol Biol* **2018**, *25*, 333-340.
59. Taylor, N. M. I.; Manolaridis, I.; Jackson, S. M.; Kowal, J.; Stahlberg, H.; Locher, K. P. Structure of the human multidrug transporter ABCG2. *Nature* **2017**, *546*, 504-509.
60. Orlando, B. J.; Liao, M. ABCG2 transports anticancer drugs via a closed-to-open switch. *Nat Commun* **2020**, *11*, 2264.
61. Stacy, A. E.; Jansson, P. J.; Richardson, D. R. Molecular pharmacology of ABCG2 and its role in chemoresistance. *Mol Pharmacol* **2013**, *84*, 655-669.
62. Telbisz, Á.; Hegedüs, C.; Özvegy-Laczka, C.; Goda, K.; Várady, G.; Takáts, Z.; Szabó, E.; Sorrentino, B. P.; Váradi, A.; Sarkadi, B. Antibody binding shift assay for rapid screening of drug interactions with the human ABCG2 multidrug transporter. *Eur J Pharm Sci* **2012**, *45*, 101-109.
63. Ozvegy-Laczka, C.; Várady, G.; Köblös, G.; Ujhelly, O.; Cervenak, J.; Schuetz, J. D.; Sorrentino, B. P.; Koomen, G. J.; Váradi, A.; Németh, K.; Sarkadi, B. Function-dependent conformational changes of the ABCG2 multidrug transporter modify its interaction with a monoclonal antibody on the cell surface. *J Biol Chem* **2005**, *280*, 4219-4227.
64. Xu, J.; Liu, Y.; Yang, Y.; Bates, S.; Zhang, J. T. Characterization of oligomeric human half-ABC transporter ATP-binding cassette G2. *J Biol Chem* **2004**, *279*, 19781-19789.
65. Yu, M.; Ocana, A.; Tannock, I. F. Reversal of ATP-binding cassette drug transporter activity to modulate chemoresistance: why has it failed to provide clinical benefit? *Cancer Metastasis Rev* **2013**, *32*, 211-227.

66. Henriksen, U.; Fog, J. U.; Litman, T.; Gether, U. Identification of intra- and intermolecular disulfide bridges in the multidrug resistance transporter ABCG2. *J Biol Chem* **2005**, 280, 36926-36934.
67. Kage, K.; Fujita, T.; Sugimoto, Y. Role of Cys-603 in dimer/oligomer formation of the breast cancer resistance protein BCRP/ABCG2. *Cancer Sci* **2005**, 96, 866-872.
68. Ni, Z.; Mark, M. E.; Cai, X.; Mao, Q. Fluorescence resonance energy transfer (FRET) analysis demonstrates dimer/oligomer formation of the human breast cancer resistance protein (BCRP/ABCG2) in intact cells. *Int J Biochem Mol Biol* **2010**, 1, 1-11.
69. Gujadhur, R.; Venkataraman, D.; Kintigh, J. T. Formation of aryl-nitrogen bonds using a soluble copper (I) catalyst. *Tetrahedron Lett* **2001**, 42, 4791-4793.

Table of Contents Graphic

